

Manuscript Number: JIB-15-0201R1

Title: Mg(II) and Ni(II) induce aggregation of poly(rA)poly(rU) to either tetra-aggregate or triplex depending on the metal ion concentration

Article Type: SI: ISMEC

Keywords: RNA; stabilisation; disproportion; non-canonical structure; quadruplex

Corresponding Author: Dr. Tarita Biver, Ph. D.

Corresponding Author's Institution: University of Pisa

First Author: Tarita Biver, Ph. D.

Order of Authors: Tarita Biver, Ph. D.; Natalia Busto, Dr; Begona Garcia, Prof; José Maria Leal, Prof; Luisa Menichetti, Dr; Fernando Secco, Prof; Marcella Venturini, Prof

Abstract: The ability of magnesium(II) and nickel(II) to induce dramatic polynucleotide conformational changes has been investigated. Kinetic experiments, spectrofluorometric titrations, melting experiments and DSC measurements concur in shedding light on a complex behaviour where the action of metal ions (Na⁺, Mg²⁺, Ni²⁺) in synergism with other operators, as the intercalating dye coralyne and temperature, all concur in the stabilisation of a peculiar polymer form. The divalent metal ions (M) fast and almost quantitatively bind to the duplex (AU) to give a RNA/metal ion complex (AUM) and then an aggregated is born by the union of two AUM units (UAUA(M₂)* tetra-aggregate). At relatively modest amounts of added divalent metal ions, the latter species evolves to the UAUM triplex after the release of a single AM strand. On the other hand, under conditions of high metal content, the UAUA(M₂)* intermediate rearranges to give a more stable tetra-aggregate. As concerns the role of coralyne (D), it is found that D strongly interact with UAUA(M₂). Also, in the presence of coralyne, divalent ions display a far enhanced ability to promote the transition of AUD into UAUD, and nickel more than magnesium, according to the efficiency sequence [Ni²⁺] >> [Mg²⁺] >> [Na⁺].



DIPARTIMENTO DI
CHIMICA E CHIMICA
INDUSTRIALE

Via Giuseppe Moruzzi, 3
56124 Pisa (Italy)
Tel. 050-2219001
E-mail: segreteria@dcci.unipi.it
PEC:dcci@pec.unipi.it
<http://www.dcci.unipi.it>

Cod. Fisc. 80003670504
P. IVA 0028682 050 1

Pisa, 16/04/2015

JIB-15-0201 Revised version

Dear Editor,

we submit to your attention the REVISED VERSION of the manuscript entitled (note that the title has been slightly revised):

Mg(II) and Ni(II) induce aggregation of poly(rA)poly(rU) to either tetra-aggregate or triplex depending on the metal ion concentration

by T. Biver, N. Busto, B. García, J.M. Leal, L. Menichetti, F. Secco, M. Venturini*

to be considered for publication in Journal of Inorganic Biochemistry (special issue for ISMEC2014).

All minor points arisen by the Reviewers have been duly taken into account (see below) and the manuscript was improved accordingly.

Appropriate corrections to the manuscript were also made according to the “Stylistic Guidelines” provided.

Best regards,

Tarita Biver

RESPONSE TO REVIEWERS

Reviewer #2

This is an interesting contributionHowever, the reading of the manuscript is not so straightforward and would need of some smoothing to arrive to a more general audience. Therefore, I would encourage the authors to make efforts in this respect.

- *Efforts have been made to smooth the manuscript and improve its readability*

Even if a drawing structure of coralyne was introduced in a previous paper of the authors, it should be also included here for clarity.

- *A Figure of the molecular structure of Coralyne has been added in the revised version of the manuscript as Figure 6 (page 9)*

There are some typos and mistakes that might be corrected. For example:

The time scale in figures 1A and 1B does not seem very different between them.

Superindexes in the abstract. In material and methods (by the way, pages are not numbered) intercalating dye able to induces. In the second paragraph after equation (5) $[Mg^{2+}]^+$

- *The indicated typos have been corrected, the manuscript was checked again to individuate other typos/mistakes and page numbering was added. As concerns the time scales in Figures 1A and 1B (and also 1C) it is true that the time scales are not different in the three Figures, but these refer to different experimental conditions.*

The sentence of the text "The two effects were analysed separately, being well separated in the time scale" refers to one single experiment: under conditions of Figure 1A the slow effect is so slow that it cannot be observed; analogously, under conditions of Figure 1C the fast effect is so fast that it cannot be observed.

Reviewer #3

The manuscript is quite interesting...provided that the following minor revisions are considered:

- The six plots of Figure 4 could be possibly merged in one figure with different line colours/styles for the different Mg concentrations.

The Suggestion of the Reviewer is undoubtedly correct and, in a first editing, the six plots of Figure 4 were indeed merged. However, despite the small differences in the y-axis, the merged figure had readability problem. In particular, in the case of the data at the lowest magnesium content, the plot compression let that the biphasic melting trend (corresponding to triplex) was no longer visible. That's why we decided for the 6 separated figures: they are less simple but ensure higher clarity of the trends.

- For a better comparison of the three plots (A, B, C) of Figure 4S, the same range of temperature axis should be used.

The same range of temperatures is now used in the three plots (A, B, C) of Figure 4S.

- Axis labels and legends of Figure 5S are difficult to see. Please try to enlarge them.

The size of Figure 5S and of the other Figures of the Supporting Information was enlarged to increase their readability.

- page 11, last row: "which possess essentially" -> "which possesses essentially"; "increase of $[Mg^{2+}]^+$ results": please delete the typo "+"; a small typo in the SI: "tetra-ggregate"

The indicated typos have been corrected; the manuscript was checked again to individuate other typos.

JIB-15-0201 RESPONSE TO REVIEWERS

Reviewer #2

This is an interesting contributionHowever, the reading of the manuscript is not so straightforward and would need of some smoothing to arrive to a more general audience. Therefore, I would encourage the authors to make efforts in this respect.

- Efforts have been made to smooth the manuscript and improve its readability

Even if a drawing structure of coralyne was introduced in a previous paper of the authors, it should be also included here for clarity.

- A Figure of the molecular structure of Coralyne has been added in the revised version of the manuscript as Figure 6 (page 9)

There are some typos and mistakes that might be corrected. For example:

The time scale in figures 1A and 1B does not seem very different between them.

Superindexes in the abstract. In material and methods (by the way, pages are not numbered) intercalating dye able to induces. In the second paragraph after equation (5) $[Mg^{2+}] +$

- The indicated typos have been corrected, the manuscript was checked again to individuate other typos/mistakes and page numbering was added. As concerns the time scales in Figures 1A and 1B (and also 1C) it is true that the time scales are not different in the three Figures, but these refer to different experimental conditions.

The sentence of the text "The two effects were analysed separately, being well separated in the time scale" refers to one single experiment: under conditions of Figure 1A the slow effect is so slow that it cannot be observed; analogously, under conditions of Figure 1C the fast effect is so fast that it cannot be observed.

Reviewer #3

The manuscript is quite interesting...provided that the following minor revisions are considered:

- The six plots of Figure 4 could be possibly merged in one figure with different line colours/styles for the different Mg concentrations.

The Suggestion of the Reviewer is undoubtedly correct and, in a first editing, the six plots of Figure 4 were indeed merged. However, despite the small differences in the y-axis, the merged figure had readability problem. In particular, in the case of the data at the lowest magnesium content, the plot compression let that the biphasic melting trend (corresponding to triplex) was no longer visible. That's why we decided for the 6 separated figures: they are less simple but ensure higher clarity of the trends.

- For a better comparison of the three plots (A, B, C) of Figure 4S, the same range of temperature axis should be used.

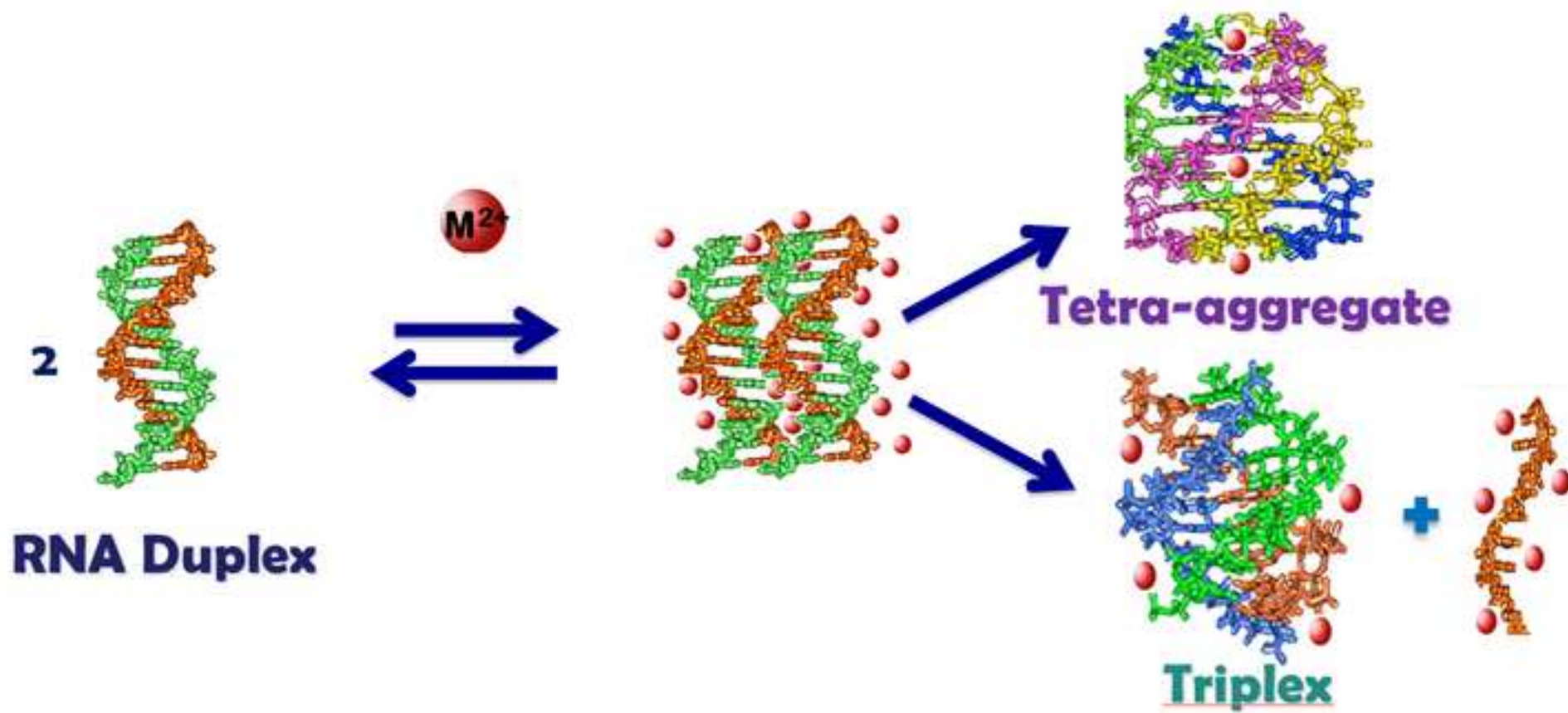
The same range of temperatures is now used in the three plots (A, B, C) of Figure 4S.

- Axis labels and legends of Figure 5S are difficult to see. Please try to enlarge them.

The size of Figure 5S and of the other Figures of the Supporting Information was enlarged to increase their readability.

- page 11, last row: "which possess essentially" -> "which possesses essentially"; "increase of $[Mg^{2+}] +$ results": please delete the typo "+)"; a small typo in the SI: "tetra-gggregate"

The indicated typos have been corrected; the manuscript was checked again to individuate other typos.



Synopsis for the Graphical abstract

Nickel and magnesium induce stabilisation of non-canonical RNA forms as tetra-aggregates or triplexes, the major form depending on metal ion concentration, temperature and/or presence of intercalating dyes. Mechanism and details of these processes are investigated.

JIB-15-0201

Highlights

- Mg^{2+} and Ni^{2+} at modest concentration induce formation of RNA triplex
- Mg^{2+} and Ni^{2+} at high concentration induce formation of RNA tetra-aggregate
- Nickel is much more effective than magnesium to induce transformations
- The transitions occur also in the presence of an intercalating dye (Coralyne)
- Dye binding affinity to the tetra-aggregate RNA form is enhanced respect to duplex

Mg(II) and Ni(II) induce duplex poly(rA)poly(rU) aggregation to either tetra-aggregate or triplex forms depending on the metal ion concentration

Tarita Biver, Natalia Busto, Begoña García, José Maria Leal, Luisa Menichetti, Fernando Secco*, Marcella Venturini

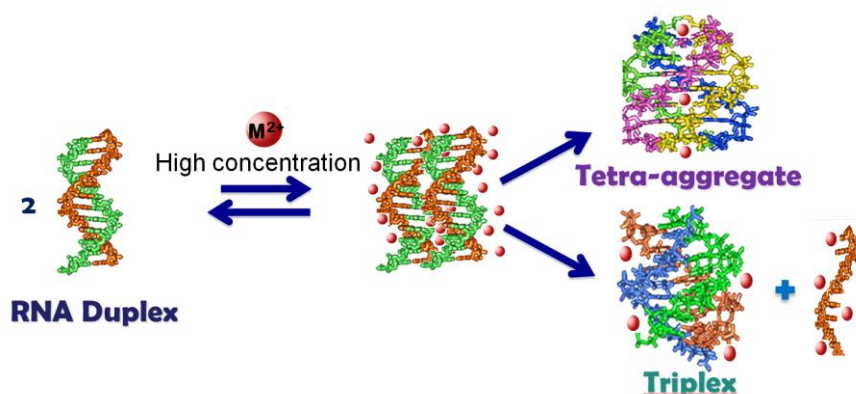
Corresponding Author: fernando.secco@unipi.it

Abstract

The ability of magnesium(II) and nickel(II) to induce dramatic polynucleotide conformational changes has been investigated. Kinetic experiments, spectrofluorometric titrations, melting experiments and DSC measurements concur in shedding light on a complex behaviour where the action of metal ions (Na^+ , Mg^{2+} , Ni^{2+}) in synergism with other operators, as the intercalating dye coralyne and temperature, all concur in the stabilisation of a peculiar polymer form. The divalent metal ions (M) fast and almost quantitatively bind to the duplex (AU) to give a RNA/metal ion complex (AUM) and then an aggregated is born by the union of two AUM units ($\text{UAUA}(\text{M}_2)^*$ tetra-aggregate). At relatively modest amounts of added divalent metal ions, the latter species evolves to the UAUM triplex after the release of a single AM strand. On the other hand, under conditions of high metal content, the $\text{UAUA}(\text{M}_2)^*$ intermediate rearranges to give a more stable tetra-aggregate. As concerns the role of coralyne (D), it is found that D strongly interact with $\text{UAUA}(\text{M}_2)$. Also, in the presence of coralyne, divalent ions display a far enhanced ability to promote the transition of AUD into UAUD , and nickel more than magnesium, according to the efficiency sequence $[\text{Ni}^{2+}] \gg [\text{Mg}^{2+}] \gg [\text{Na}^+]$.

Keywords RNA, stabilisation, disproportion, non-canonical structure, quadruplex

Graphical Abstract



Nickel and magnesium induce stabilisation of non-canonical RNA forms as tetra-aggregates or triplexes, the major form depending on metal ion concentration, temperature and/or presence of intercalating dyes. Mechanism and details of these processes are investigated.

Highlights

- Mg^{2+} and Ni^{2+} at modest concentration induce formation of RNA triplex
- Mg^{2+} and Ni^{2+} at high concentration induce formation of RNA tetra-aggregate
- Nickel is much more effective than magnesium to induce transformations
- These transitions occur also in the presence of an intercalating dye
- Dye binding affinity to the tetra-aggregate RNA form is enhanced respect to duplex

Introduction

It is now clear that the occurrence of non-canonical forms of polynucleotides, such as triple or quadruple helices, is fundamental in a wide number of biochemical reactions [1-4]. As concerns triplexes, their use in the “antigen” and/or “antisense” strategies is also a major interest [5-7]. On the other hand, quadruple helices are suspected to occur in the genome [8] and to constitute important regulators of both DNA and RNA polynucleotides [9]. The three-dimensional architecture of the above structures depends also on the presence metal ions. Given the negative charge of the phosphate-sugar backbone, positively charged counter-ions are crucial for stabilisation [10, 11]. There is now substantial evidence that metal ions bind to specific sites [12, 13], stabilizing local motifs and positioning themselves correctly to aid (or even enable) a catalytic mechanism, as for instance in ribozymes. The effect exerted depends not only on the concentration but on the type of metal ion involved. The formation of triplexes can also be induced by an intercalating dye: we have recently demonstrated that coralyne is able to induce triple helix formation in poly(rA)poly(rU), through an intermediate step that involves formation of a tetra-aggregate [14]. As regards the synthetic RNA poly(rA)poly(rU), literature data are limited to the thermodynamic aspects of duplex-triplex transitions induced by Mg^{2+} and Ni^{2+} ions at low concentration [15-17]. In the present work, we have analysed the kinetic aspects of the transition induced by relatively high Mg^{2+} and Ni^{2+} in order to acquire information about the binding mechanism and the conditions that favour the stabilization of different RNA multiplexes. The possible synergistic effects induced by the presence of coralyne and the binding of coralyne to the non-canonical forms are also investigated in order to get light on this complex system.

Materials and methods

Materials Ultra-pure water from a Millipore S.A. 670120 water purification system was used throughout. All reagents (as NaCl, MgCl₂ and NiCl₂) were analytical grade and were used as received. The pH measurements were done using a Metrohm pH-meter. All solutions were kept at pH = 7.0 using a 0.01M Sodium Cacodylate buffer (NaCac = (CH₃)₂AsO₂Na). Ionic strength was adjusted to the desired value by suitable addition of NaCl, MgCl₂ or NiCl₂ (all from Sigma). The stock solutions of the salts were obtained by dissolving appropriately weighted amounts in water. Poly(rA)poly(rU) and poly(rU) (lyophilised sodium salts, Sigma) were dissolved into water. Their concentration was measured spectrophotometrically using the appropriate molar extinction coefficient (ϵ): for poly(rA)poly(rU) $\epsilon = 14900 \text{ M}^{-1}\text{cm}^{-1}$ at 260 nm, pH = 7, I = 0.10 M (NaCl) and for poly(rU) $\epsilon = 8900 \text{ M}^{-1}\text{cm}^{-1}$ at 260 nm, pH = 7, I = 0.10 M (NaCl) as obtained from the sample certificate. The molar concentration of the polynucleotide is indicated as C_P. The working solutions are kept at 4°C and used within a week. From now on poly(rA)poly(rU) will simply be denoted as poly(A)poly(U) or AU.

Coralyne, a fluorescent intercalating dye able to induces triple helix formation (poly(rA)₂poly(rU) or UAU) in poly(rA)poly(rU) [14] was the pure solid (> 99.9%) from Sigma. Its solutions were prepared by dissolving weighted amounts in MilliQ water (MW = 417.89). Both solid and solutions are kept in the dark at 4°C; aqueous solutions are used within two days, the molar concentration of the dye is indicated as C_D.

Methods UV-vis spectrophotometry The kinetic measurements have been done using a Perkin-Elmer Lambda 35 double beam spectrophotometer. The rate of the reaction occurring upon addition of MgCl₂ to solutions of poly(A)poly(U) was measured by monitoring the variation of the absorbance signal at 260 nm with time. Classical spectrophotometric technique could be employed thanks to the slowness of the processes observed (minute's time range). The dead time (interval between mixing and start of recording) is estimated to be as low as 5 s.

Spectrofluorometry Fluorescence measurements were performed using a Perkin Elmer LS55 spectrofluorometer with temperature control to within $\pm 0.1^\circ\text{C}$. In the coralyne/RNA spectrofluorometric titrations, increasing amounts of the polymer are added to the dye solution directly in the spectrofluorometric cell (both solutions being kept at the same desired pH and ionic strength I). Concerning titrations of the poly(A)poly(U)/coralyne system with salts, increasing amounts of the metal ion solution were added to a polymer solution present in the cell at a given poly(A)poly(U)/coralyne ratio. In another set of experiments, a coralyne solution containing a given concentration of NaCl, MgCl₂ or NiCl₂, was titrated with poly(A)poly(U) containing the identical metal ion concentration. Note that the spectrofluorometric approach and the high fluorescence

efficiency of coralyne enable very low concentration of the intercalating dye be used (10^{-7} M) so that dye self-aggregation problems are avoided [18]. The additions were made using a Hamilton syringe connected to a micrometric screw that enabled volumes as small as 0.166 μ L to be added. The cuvette is thermostatted within $\pm 0.1^\circ\text{C}$.

Melting experiments The melting experiments were performed using a Hewlett-Packard 8452A (Agilent) single beam, diode array apparatus. The path length of the cuvettes used is 1 cm and they are thermostatted within $\pm 0.1^\circ\text{C}$. The absorbance variation with temperature at 260 nm is measured using a scanning rate of $0.2^\circ\text{C}/\text{min}$ and 1 min stabilisation time for each step. The melting temperature T_m is obtained by the first derivative of the melting plot. In the experiments on poly(A)poly(U) at different metal ion content the polynucleotide concentration is kept at 1.7×10^{-5} M. The desired amount of MgCl_2 was added directly in the spectrophotometric cell containing the poly(A)poly(U) solution and the mixture was left to equilibrate for 2h. As regards the experiments in the presence of coralyne, $C_D = \text{constant} = 1.7 \times 10^{-5}$ M and the polynucleotide concentration is varied to reach the desired C_D/C_P ratio. The dye/polymer mixture was left to reach equilibrium for 2h before starting the melting experiment.

Circular Dichroism (CD) CD spectra (200 \div 700 nm, 1.0 cm path length) were registered using a MOS-450 Biologic (Claix, France) apparatus equipped with $\pm 0.1^\circ\text{C}$ temperature control. CD titrations were done by adding increasing amounts of dye to the polymer directly in the cell.

Differential Scanning Calorimetry (DSC) Differential Scanning Calorimeter (DSC) data were obtained using a Setaram micro DSC III differential scanning calorimeter. We measured the thermodynamic parameters for the denaturalisation of poly(A)poly(U) ($C_P = 2.5 \times 10^{-4}$ M) at different Mg^{2+} contents and of poly(A)poly(U)/coralyne at different Na^+ contents. The volume of the solution was 850 μ L and the scan rate $1^\circ\text{C}/\text{min}$. All solutions were degasified for 15 min with a TA instruments apparatus before filling the cell. Data were analysed using the NanoAnalyze 2.0 software.

Results – poly(A)poly(U)/metal ions.

Kinetic study of the poly(A)poly(U)/magnesium system

In order to analyse the influence of poly(A)poly(U) or magnesium on the kinetics of the system, two different sets of experiments were done: (A) variation of the poly(A)poly(U) concentration, C_P , at constant Mg^{2+} ion concentration and (B) variation of $[\text{Mg}^{2+}]$ at constant C_P . Note that, in the here presented work, a wide range of metal ion content was used (from 2×10^{-3} M to 0.2 M). At $C_P = 1.8 \times 10^{-5}$ M and $[\text{Mg}^{2+}] = 1.2 \times 10^{-2}$ M two kinetic effects of different amplitude are observed (Figure 1B). The first (fast) one (absorbance decrease) is predominant when $[\text{Mg}^{2+}] < 1.2 \times 10^{-2}$ M (Figure

1A), whereas the second (slow) one (absorbance increase) prevails if $[Mg^{2+}] > 5.5 \times 10^{-2}$ M (Figure 1C). The two effects were analysed separately, being well separated in the time scale.

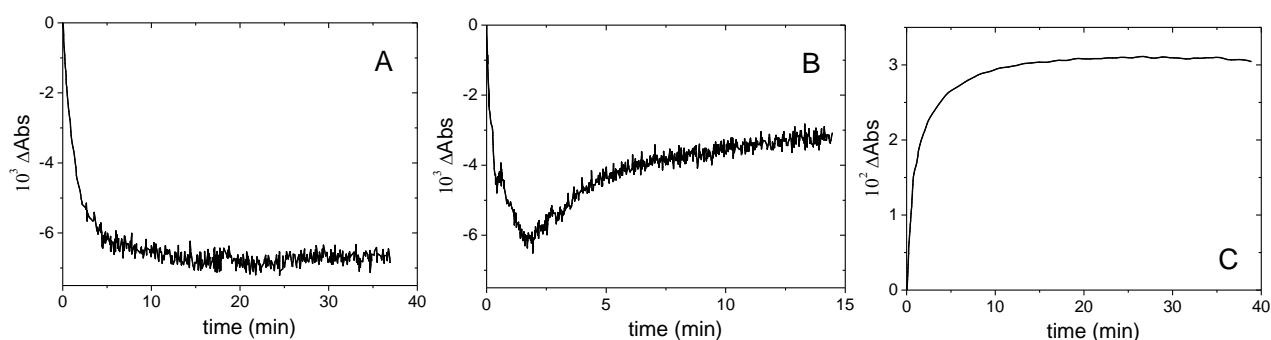


Figure 1. Kinetic curves for the poly(A)poly(U)/ Mg^{2+} system; $C_P = 1.8 \times 10^{-5}$ M, $[NaCac] = 0.01$ M, $pH = 7.0$, $\lambda = 260$ nm, $T = 25$ °C. (A) $[Mg^{2+}] = 6.7 \times 10^{-3}$ M, (B) $[Mg^{2+}] = 1.2 \times 10^{-2}$ M, (C) $[Mg^{2+}] = 0.2$ M.

Fast effect – Absorbance decrease The kinetic effect connected to the absorbance decrease was analysed using the initial rate approach. The absorbance variation in time is evaluated by the slope of the initial portion of the curve. The slope value ($Abs\ s^{-1}$) was converted to a variation of concentration in time using the molar extinction coefficient of poly(A)poly(U). The reaction order respect to the polymer (experiments at $[Mg^{2+}] = \text{constant}$ and different C_P) turned to be equal to one (Figure 2A, slope is 0.9 ± 0.1). Note that in these experiments the overall ionic strength is controlled by the contribution of magnesium and is, therefore, constant. The determination of the reaction order respect to magnesium, instead, required experiments where the metal ion concentration changes (Figure 2B). Thus, a correction is needed to account for the dependence of the initial rate on the ionic strength (see Discussion).

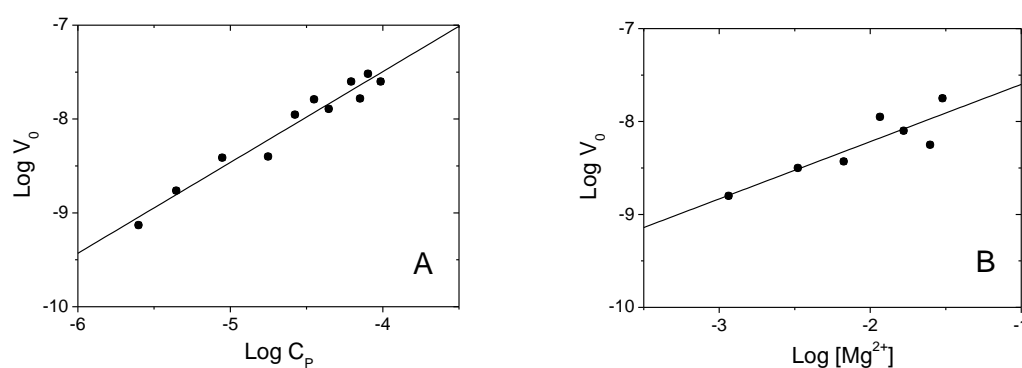


Figure 2. Fast effect for the poly(A)poly(U)/ Mg^{2+} system, $[NaCac] = 0.01$ M, $pH = 7.0$, $T = 25$ °C: dilogarithmic plot of initial rate (V_0) dependence (A) on the polymer content C_P at $[Mg^{2+}] = 6.7 \times 10^{-3}$ M, (B) on the magnesium content at $C_P = 1.8 \times 10^{-5}$ M.

Slow effect – Absorbance increase The kinetic curves in the 5.5×10^{-2} M - 0.2 M range of $[\text{Mg}^{2+}]$ were also analysed using the initial rate method. Under these experimental conditions (high metal ion content) the fast reaction is so fast that it can be intended as a pre-equilibrium; the data obtained will be thus relative to the effect connected with absorbance increase.

The dilogarithmic graph shown in Figure 3A, where data at constant $[\text{Mg}^{2+}]$ and variable C_P are plotted, yields the reaction order respect to RNA. This turned to be equal to two (slope is 1.8 ± 0.1). As concerns magnesium, experiments at constant C_P and different $[\text{Mg}^{2+}]$ (from 0.12 M to 0.61 M) were also done (Figure 3B). However, due to the non-constant dominant magnesium content, the global ionic strength of the medium is not constant in the different experiments. An ionic strength effect correction is therefore needed (see Discussion).

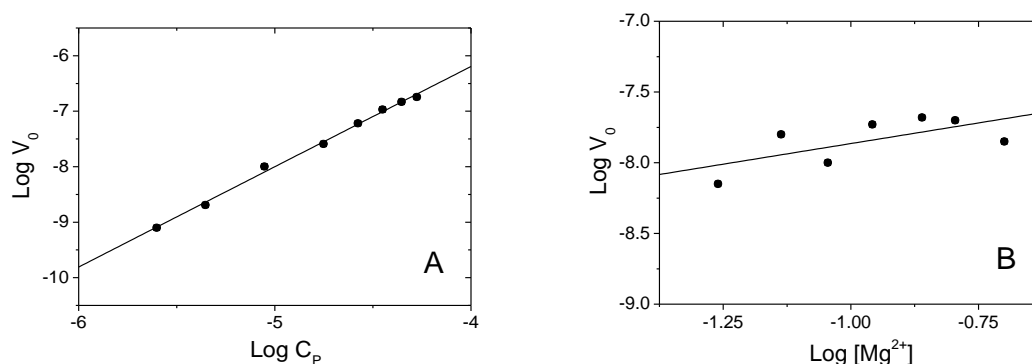


Figure 3. Slow effect for the poly(A)poly(U)/ Mg^{2+} system, $[\text{NaCac}] = 0.01$ M, $\text{pH} = 7.0$, $T = 25^\circ\text{C}$: dilogarithmic plot showing the initial rate (V_0) dependence (A) on the polymer content C_P at $[\text{Mg}^{2+}] = 0.138$ M, (B) on the magnesium content at $C_P = 1.8 \times 10^{-5}$ M.

Kinetic study of the poly(A)poly(U)/nickel system

The poly(A)poly(U)/ Ni^{2+} system was analysed by the same method used for the poly(A)poly(U)/ Mg^{2+} system. As for magnesium, also for nickel two distinct kinetic effects of opposite amplitude are observed upon addition of metal ion to the polynucleotide (Figure 1S-B of the Supporting Information). In the case of nickel, however, significantly lower metal ion concentrations were needed to obtain similar experimental evidences (from 1.5×10^{-3} M to 1.5×10^{-2} M). This result is in agreement with the higher efficacy of Ni^{2+} respect to Mg^{2+} to produce effects on the polynucleotides structure [19]. For $[\text{Ni}^{2+}] < 1.5 \times 10^{-3}$ M the fast kinetic effect, connected to absorbance increase, is dominating (Figure 1S-A). The initial rate evaluation and relevant dilogarithmic analysis (Figure 2S) yielded a reaction order equal to one with respect to

poly(A)poly(U) and zero with respect to the metal ion. For $[\text{Ni}^{2+}] \geq 1.5 \times 10^{-3} \text{ M}$ the slow kinetic effect, connected to absorbance increase, is dominating (Figure 1S-C). Initial rate analysis and relevant dilogarithmic plots (Figure 3S) indicate that the reaction order with respect to polymer is two and with respect to nickel is zero. Note that in the case of nickel the ionic strength is so low that no ionic strength correction is needed. On the whole, the results obtained for nickel are superimposable to those of magnesium with the difference that less than at least one order of magnitude metal ion is needed in case of Ni^{2+} for producing same effects.

Thermal denaturation experiments

Figure 4 shows the thermal denaturation profiles obtained for the poly(A)poly(U)/ Mg^{2+} system at different magnesium contents. If $3.5 \times 10^{-3} \text{ M} \leq \text{Mg}^{2+} \leq 0.02 \text{ M}$, two distinct transitions are present. The amplitude of the transition and melting temperature, T_m , values of the first transition does increase as the metal ion concentration is raised, whereas the second transition (ca. 80°C) seems to be insensitive to $[\text{Mg}^{2+}]$.

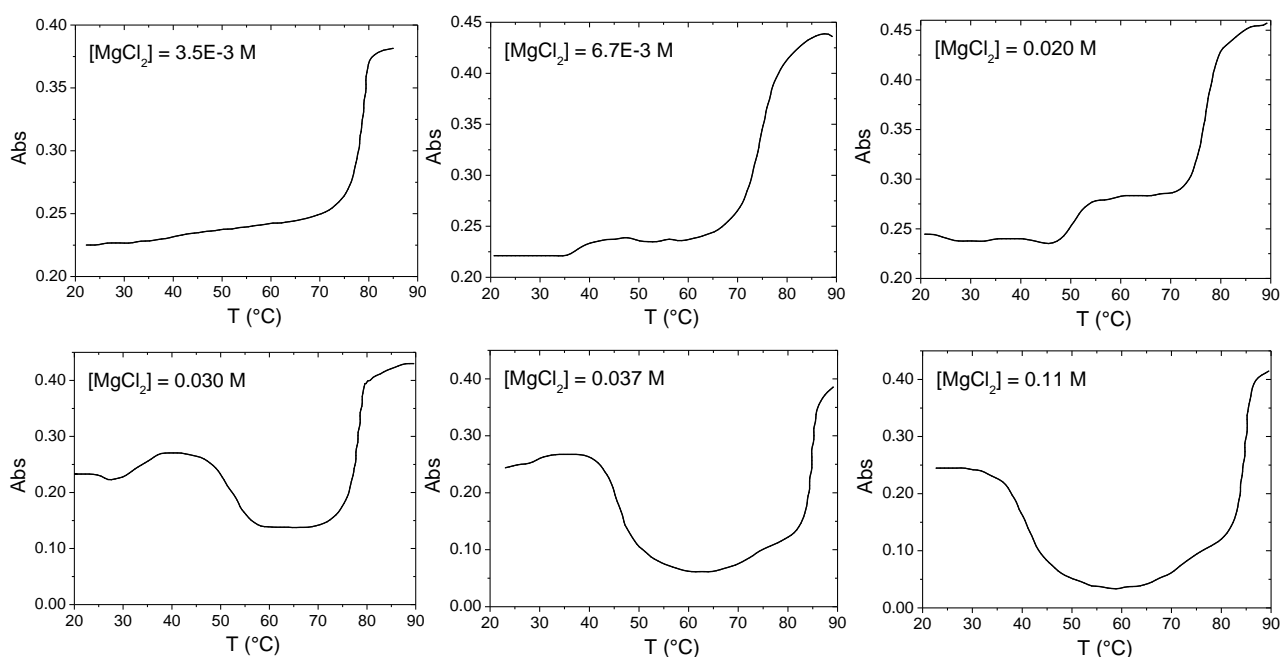


Figure 4. Melting profiles for the poly(A)poly(U)/ Mg^{2+} system at different magnesium content; $C_P = 1.7 \times 10^{-5} \text{ M}$, $[\text{NaCac}] = 0.01 \text{ M}$, $\text{pH} = 7.0$, $\lambda = 260 \text{ nm}$.

The melting profiles significantly change at $[\text{Mg}^{2+}] > 0.02 \text{ M}$. The values of the initial absorbance are slightly higher compared to the values displayed at lower values of the magnesium concentration (ca. 0.25 for $[\text{Mg}^{2+}] \geq 0.020 \text{ M}$ vs. ca. 0.225 for $[\text{Mg}^{2+}] \leq 6.7 \times 10^{-3} \text{ M}$). Moreover, the general trend is different and is characterised by a dramatic decrease of the absorbance that reaches

a minimum. After an initial slight absorbance increase a deep decrease of the signal occurs, the amplitude of the latter major effect being higher the higher the $[\text{Mg}^{2+}]$ concentration. Only for $T > 60^\circ\text{C}$, a biphasic trend, similar to that observed for $[\text{Mg}^{2+}] < 0.02 \text{ M}$ could be observed. On the other hand, the temperature corresponding to the maximum related to the initial modest absorbance increase is lower the higher the metal ion content, until it disappears ($T < 20^\circ\text{C}$) for $[\text{Mg}^{2+}] = 0.11 \text{ M}$.

Circular Dichroism (CD) A circular dichroism titration was done where increasing amounts of MgCl_2 are added to a poly(A)poly(U) solution. The CD spectra obtained are shown in Figure 5A. The molar ellipticity in the UV region, typical of the polymer conformation, retains its band shape as $[\text{Mg}^{2+}]$ stays below 0.024 M but shows non negligible decrease as $[\text{Mg}^{2+}] \geq 0.053 \text{ M}$. Moreover, the maxima of the dichroic bands display a frequency shift as shown in Figure 5B with a minimum corresponding to about $[\text{Mg}^{2+}] = 0.11 \text{ M}$. This biphasic behaviour is in agreement with kinetic and thermal denaturation findings.

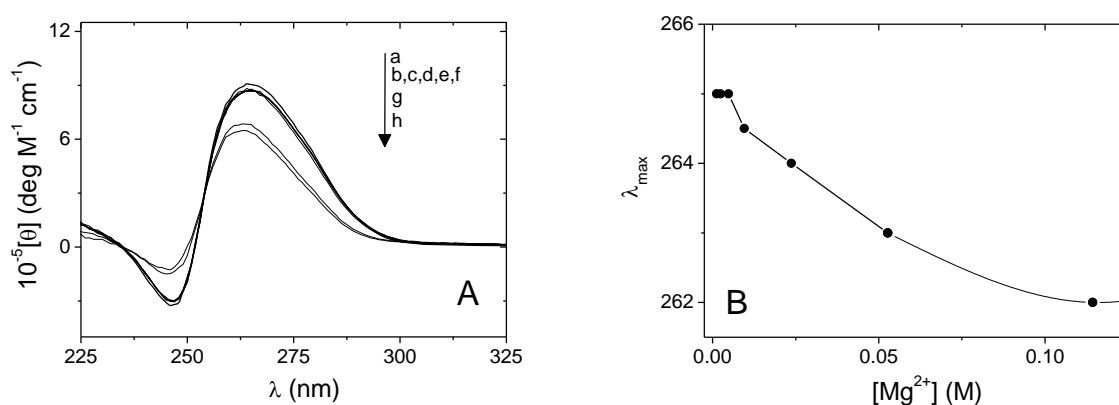


Figure 5. CD titration of poly(A)poly(U) with MgCl_2 ; $C_P = 1.5 \times 10^{-5} \text{ M}$, $\text{pH} = 7.0$, 25°C . (A) CD curves when $[\text{MgCl}_2]$ increases from 0 M to 0.5 M as indicated by the arrow: (a) 0 M , (b) $1.2 \times 10^{-3} \text{ M}$, (c) $2.4 \times 10^{-3} \text{ M}$, (d) $4.8 \times 10^{-3} \text{ M}$, (e) $9.5 \times 10^{-3} \text{ M}$, (f) 0.024 M , (g) 0.053 M , (h) 0.11 M . (B) Position of the maximum of the positive dichroic band as a function of the magnesium content (line to drive the eye).

Differential scanning calorimetry (DSC)

The thermal stability of poly(A)poly(U)/ Mg^{2+} at different magnesium content was qualitatively analysed by DSC. The relevant thermograms are shown in Figure 4S of the Supporting Information. A single endothermic transition is observed, in agreement with the occurrence of a denaturation process. The temperature of the transition is $86.1 \pm 0.2^\circ\text{C}$ independently of the Mg(II) content.

Accordingly, the ΔH and ΔS values are also (within the experimental error) coincident at the different $[\text{Mg}^{2+}]$, being $\Delta H = 27 \pm 2 \text{ KJ}\cdot\text{mol}^{-1}$ and $\Delta S = 75 \pm 5 \text{ J}\cdot\text{mol}^{-1}\cdot\text{K}^{-1}$ ($[\text{NaCac}] = 0.01 \text{ M}$, $\text{pH} = 7.0$, $T = 25^\circ\text{C}$).

Results – poly(A)poly(U)/coralyne/metal ions

It has already been shown that coralyne interacts with poly(A)poly(U) in a complex way where triple helix formation is induced [14, 20]. In the present study we have investigated the influence of metal ions on the poly(A)poly(U)/coralyne system and the ability of coralyne to interact with the poly(A)poly(U)/metal ion system.

Spectrofluorimetric titrations

Spectrofluorometric titrations of coralyne with poly(A)poly(U) were done in aqueous solutions containing different concentrations of NaCl ranging between 0.020 M to 1.0 M (Figure 5S). The binding isotherms are biphasic independently of the salt content: a fluorescence decrease is displayed in the first phase whereas the second phase is related to a fluorescence increase. On the other hand, the slope of the branches and the position (C_P value) at which the minimum is reached both depend on the added salt content. A mixture of poly(A)poly(U) and coralyne (in 0.1M NaCl and 0.01M NaCac, $\text{pH} = 7.0$) at C_P/C_D equal to the minimum of the binding isotherm ($I = 0.11\text{M}$, $C_D/C_P = 0.23$, $C_D = 6.5 \times 10^{-7}$, Figure 5S) is prepared. If NaCl is added to this mixture, the fluorescence of the system increases (Figure 6A). The experiment is repeated, using the same starting mixture but using either magnesium (Figure 6B) or nickel (Figure 6C) ions. The observed effect of fluorescence increase is qualitatively the same, but lower quantities of MgCl_2 and much lower amounts of NiCl_2 with respect to sodium are needed to reach the plateau.

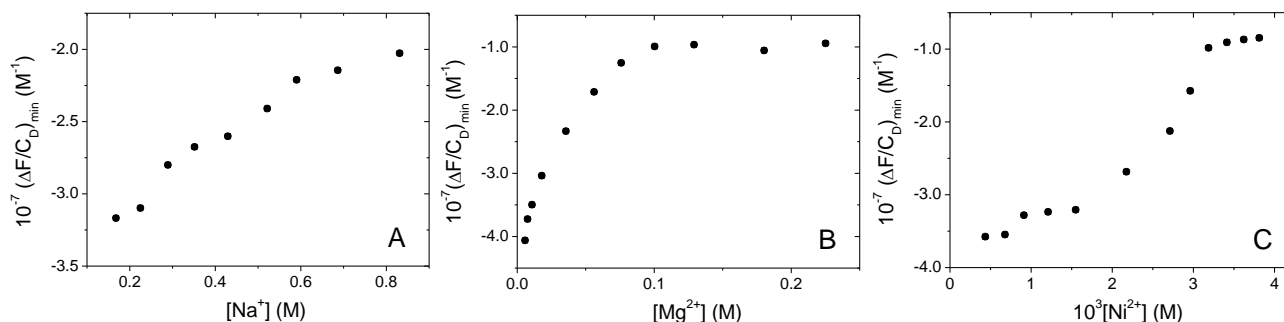


Figure 6. Trends showing fluorescence increase when increasing amounts of metal ions are added to a poly(A)poly(U)/coralyne mixture (C_P/C_D chosen to ensure maximum formation of the polymer/dye complex); $C_D = 6.5 \times 10^{-7} \text{ M}$, $C_P = 2.8 \times 10^{-5} \text{ M}$, $\text{pH} = 7.0$, $T = 25^\circ\text{C}$, $\lambda_{\text{exc}} = 420 \text{ nm}$, $\lambda_{\text{em}} = 470 \text{ nm}$; (A) $[\text{Na}^+]$, (B) $[\text{Mg}^{2+}]$, (C) $[\text{Ni}^{2+}]$.

In a different experiment a coralyne/Mg²⁺ solution is used to titrate a poly(A)poly(U)/Mg²⁺ mixture where the magnesium ion is 0.3M i.e. higher than that employed in the experiment of Figure 1C. The poly(A)poly(U)/Mg²⁺ mixture is left to equilibrate for 1h before to begin the titrations. Therefore, in this experiment, we analysed the binding of the coralyne to the peculiar polymer conformation induced by very high metal ion content. The binding isotherm obtained is shown in Figure 7A. Figure 7B shows the analogous experiment, where MgCl₂ 0.3M is replaced by NiCl₂ 0.048M. The trends found in both cases reveal the occurrence of strong binding of coralyne dye to the polymer also in these conditions.

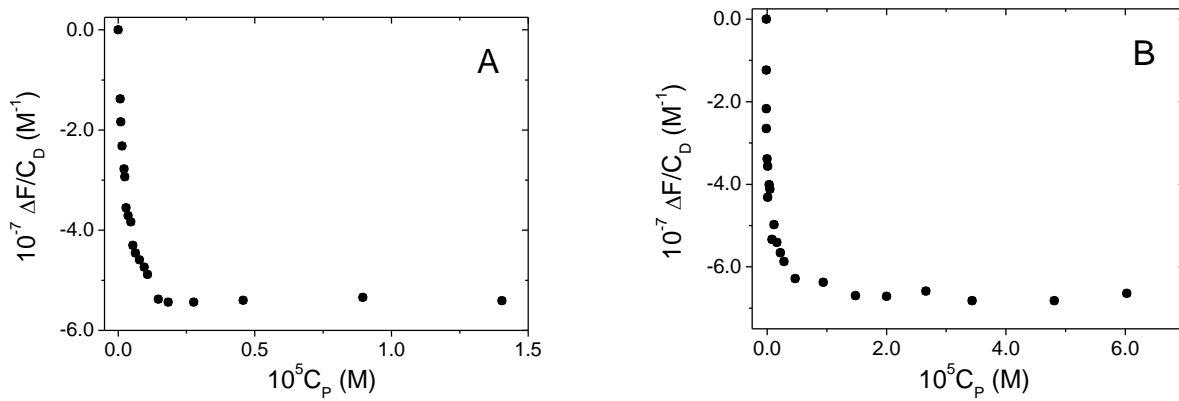
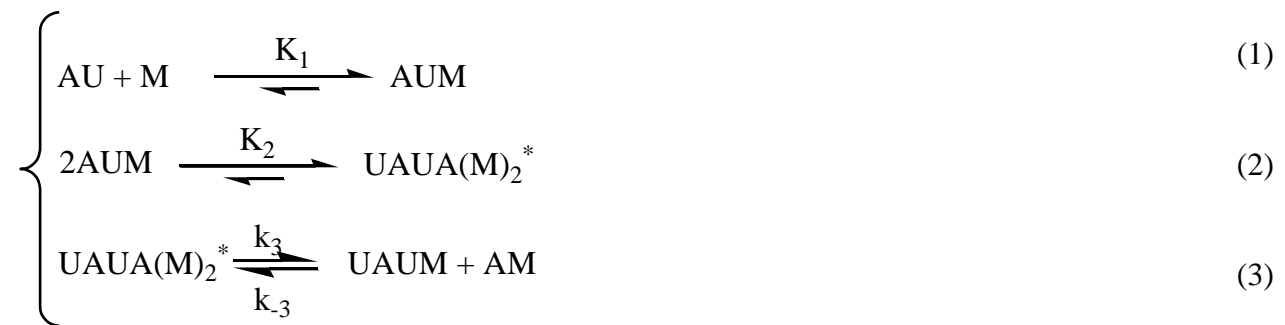


Figure 7. Binding isotherm for the poly(A)poly(U)/coralyne system (A) in MgCl₂ 0.3M, (B) in NiCl₂ 0.048M; C_D = 6.5×10⁻⁷ M, pH = 7.0, T = 25°C, λ_{exc} = 420 nm, λ_{em} = 470 nm.

Discussion

Poly(A)poly(U)/Mg²⁺ and Poly(A)poly(U)/Ni²⁺

On the basis of the results of the kinetic and melting studies the following reaction scheme is proposed (equations 3-5) to represent the time course of the first kinetic phase shown in Figure 1A.



Here, M is the divalent metal ion (Mg²⁺ or Ni²⁺) and AUM a poly(A)poly(U)/metal ion complex which possess essentially the characteristics of an electrostatic ion pair. UAUA(M)₂* is an

aggregate formed by the union of two AU double strands which are held together by electrostatic Mg^{2+} bridges. UAUM is a triplex species born after the release of a single AM strand from $UAUA(M_2)^*$. It should be noticed that the amplitudes of the fast phase were found to decrease as $[Mg^{2+}]$ is increased (Figure 6S), meaning that sequence (1)-(3) represents an equilibrium process. The equilibrium constant of reaction (1) is known from the literature and is relatively high ($K_1 \approx 8 \times 10^3$ for magnesium in $[Na^+] = 0.01M$ [21]). Therefore, in the presence of relatively high amounts of metal ion, reaction (1) can be supposed to be shifted towards the products. The AUM complex is majority under the experimental conditions used and forms so fast [22] that it will be already formed at the start of the spectrophotometric experiments.

In the presence of low amounts of divalent metal ions a triplex, UAUM, is formed according to reaction (3). This transformation is possible as the aggregate form $UAUA(M_2)^*$ is unstable and evolves thus to the triplex through the expulsion of a poly(A) single strand. This hypothesis agrees with the finding that low magnesium contents can stabilise the poly(U)poly(A)poly(U) triple helix [17]. On the basis of reaction scheme (1-3) it can be demonstrated (see the Supporting Information) that $V_0 = k_3 C_P / 2$. The reaction order is one respect to polymer in agreement with experimental finding. As regards magnesium, it has been found that the initial rate increases as the metal ion concentration (and thus the ionic strength) is raised with a slope of the dilogarithmic plot that is lower than one (slope in Figure 2B is 0.6 ± 0.1). The increasing trend indicates interaction of reagents of same sign and agrees with the proposed mechanism. In fact, being reaction (1) very fast and almost quantitative and reaction (3) insensitive to the salt content, reaction (2) will dominate the electrostatic behaviour. Any attempt to correct the ionic strength contribution (using for instance the Debye-Hückel limiting law or Guggenheim equation [24]) reduces the slope of the plot of Figure 2B and brings the order of reaction respect to magnesium equal to zero in agreement with the rate equation derived by the proposed reaction scheme.

In the presence of high amounts of metal ions, reaction (3) is repressed and a new reaction occurs (reaction (4)) which corresponds to the rate-determining conversion of the unstable species $UAUA(M_2)^*$ to the more stable form $UAUA(M)_2$. The hypothesis of the formation of an aggregate is in agreement with previous observations that suggest the divalent ions (and in particular magnesium) are able to strengthen inter-strand interactions in poly(A) [23]. It has also been demonstrated that an increase of the Mg^{2+} concentration in poly(A)/ Mg^{2+} mixtures induces aggregation/condensation processes of the single strand that results in absorbance increases [23].



Reaction (4) represents an equilibrium because the analysis of the dependence of the relaxation time on the polymer concentration yields a straight line with a positive intercept (Figure 7S) which indicates the occurrence of the reverse step.

The kinetic equation for the (1)-(2)-(4) system is (see Supporting Information for derivation) is the following

$$V_0 = k_2' K_2 \frac{C_P^2 K_1^2 [M]^2}{(1 + K_1^2 [M]^2 + 2K_1 [M])} \quad (5)$$

Being under the experimental conditions used $K_1^2 [M]^2 \gg 1 + 2K_1 [M]$ one obtains that $V_0 = k_2' K_2 C_P^2$. The reaction order is therefore two with respect to polymer and zero to metal ion, in agreement with experimental findings. As concerns magnesium, note indeed that the above discussion on the data at low metal ion content also holds in the case of the data at high magnesium content: correction for the ionic strength effect brings the order of reaction respect to magnesium equal to zero.

The above discussed mechanism is corroborated by the analysis of the melting profiles. The two transitions observed at low magnesium content agree with the presence of a triple helix as a major component at 25°C (Figure 4). In the first transition the poly(U)poly(A)poly(U) converts to the duplex by releasing a poly(U) single strand. The amplitude and melting temperature for this step depends on the Mg^{2+} concentration: it is higher the higher the content in divalent metal ion until $[Mg^{2+}] \approx 0.02M$, in agreement with an increased stabilisation of the triplex. The second transition corresponds to dissociation to give poly(A) and poly(U) single helices and is insensitive to the presence of Mg^{2+} ions (ca. 80 °C at every $[MgCl_2]$ employed). This finding indicates negligible interaction of the duplex with the metal ion at this temperature. The change of the melting profiles at higher magnesium concentrations is in agreement with the presence of an aggregate. The higher initial absorbance value reveals that, already at 20°C and $[Mg^{2+}] = 0.025 M$ non-negligible amounts of $UAUA(M)_2$ are formed. The aggregate is initially present (20°C) in a mixture with AUM but aggregation is favoured by the temperature increase and reaches its maximum extent at 45°C. An increase of $[Mg^{2+}]$ results in a shift of the maximum aggregation toward lower temperatures. Actually, aggregation is favoured by this metal ion to such a level that, for $[Mg^{2+}] = 0.11 M$, the aggregate is the prevailing form already at 20°C. Accordingly, it has been observed [23] for poly(A)/ Mg^{2+} that temperature increase favours single strands condensation. Once the aggregate formed, a further temperature increase will produce the disproportion of the aggregate form into

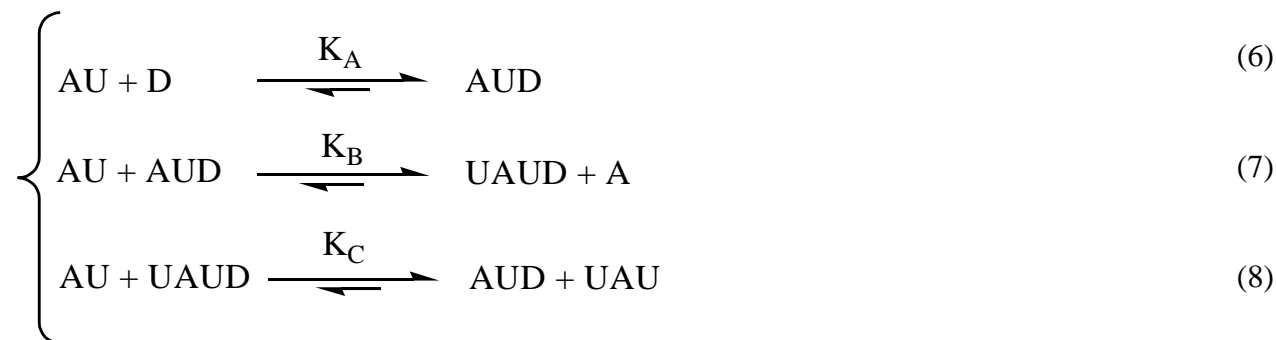
UAU triplex and U single strand. Under these conditions the absorbance reaches a minimum, as observed both in melting and in kinetic experiments. This process also occurs at lower temperatures the higher is the metal ion content. After this stage, the trend will follow the typical biphasic trend of a triple helix, with the final dissociation occurring again around 80°C. The value of $T_m = 80^\circ\text{C}$ corresponds to the denaturation of the triplex in the absence of salts [14].

CD results confirm a picture where the metal ion content shifts the equilibria towards different RNA forms. For $[\text{Mg}^{2+}] < 0.01 \text{ M}$ the triplex is majority, whereas increasing amounts of the metal ion stabilise a more aggregated (tetra-aggregate) form. The transitions duplex – triplex – tetra-aggregate are accompanied by a loss of order (ellipticity decrease) that is negligible in the case of duplex – triplex transition, whereas is much more significant in the case of the step leading to the formation of the aggregate (Figure 5).

In the case of DSC a single transition has been observed. This is likely the more energetic one and, being its ΔH value positive, it should represent the duplex to single strand transition. This result suggests that the other transitions (triplex-duplex and aggregate-triplex) are characterised by a lower enthalpic content. The constant ΔH value found under different MgCl_2 is in agreement with the fact that in all cases the same transition is observed. Note that in this study the DSC approach is scarcely sensitive to the complexity of the system. This can be said also taking into account that the use of C_P concentrations similar to that of melting experiments ($C_P = 1.7 \times 10^{-5} \text{ M}$) the amplitude of the DSC graphs would had been 15 times lower respect to that of the experiment reported in Figure 4S and the experiments under these conditions would had been affected by high noise and error.

Poly(A)poly(U)/coralyne/metal ions

The biphasic isotherms obtained at different NaCl content from the spectrophotometric titrations (Figure 8S) were analysed on the basis of the already proposed mechanism [14] shown below



In this mechanism the interaction between poly(A)poly(U) (AU) and coralyne (D) produces first the formation of the AUD complex that will then interact with AU to produce a triplex/coralyne (UAUD); in the final step a fast exchange of D produces the release of free UAU triplex. On the

basis of this reaction mechanism the equation (9) was derived, that is used to fit the experimental trend. The values of the equilibrium constants obtained for different NaCl contents are collected in Table 1S of the Supporting Information.

$$\frac{F}{C_D} = \varphi_D + \frac{\Delta\varphi_A K_A [AU] + \Delta\varphi_B [AU] \sqrt{K_A K_B / ([D] + K_C / K_A)}}{1 + K_A [AU] + [AU] \sqrt{K_A K_B / ([D] + K_C / K_A)}} \quad (9)$$

In equation (9) φ_D is the optical parameter for coralyne, $\Delta\varphi_A = (\varphi_{AUD} - \varphi_D)$ and $\Delta\varphi_B = (\varphi_{UAUD} - \varphi_D)$. The decrease of fluorescence until the minimum in the binding isotherm corresponds to formation of AUD, whereas the fluorescence increase is related to the reactions (7) and (8).

In agreement with the Record theory [24] $\text{Log}K_A$ depends linearly on $\text{Log}[\text{Na}^+]$ with a slope that corresponds to the number of Na^+ ions displaced from the polynucleotide upon binding of a dye molecule. This slope, for the present system, is equal to ca. 0.5, indicating that two molecules of coralyne are needed to displace one sodium ion.

The fact that addition of NaCl to a mixture of poly(A)poly(U) and coralyne at C_P/C_D equal to the minimum of the binding isotherm (where AUD is majority) produces a fluorescence increase can be explained on the basis of equation (7). This means that sodium ions favour the disproportion reaction and triple helices formation. Reaction (10) could also be possible as an alternative to equation (7), but the latter will be dominant under conditions of polymer excess.



Sodium, magnesium or nickel ions show different ability to drive equilibrium towards triplex formation (Figure 6). The titrations of coralyne with poly(A)poly(U) in the presence of high metal ion amount (Figure 7), represent, on the basis of the mechanism (1)-(2)-(4), the binding affinity of coralyne to the $\text{UAUA}(\text{M})_2$ aggregate. These equilibria can be quantitatively analysed using equation (11).

$$\frac{C_D C_P}{\Delta F} + \frac{\Delta F}{\Delta\varphi^2} = \frac{1}{K\Delta\varphi} + \frac{(C_P + C_D)}{\Delta\varphi} \quad (11)$$

where K is the equilibrium constant for the binding of the dye (D) to the polymer aggregate ($\text{UAUA}(\text{M})_2$, P) to give the $\text{DUAUA}(\text{M})_2$ (PD) complex, $\Delta F = F - \varphi_D C_D$, $\Delta\varphi = \varphi_{PD} - \varphi_D$ and the $\Delta F/\Delta\varphi^2$ term is not initially known but can be calculated using an iterative procedure [25]. The

relevant plots are shown in Figure 6S; the ratio between slope and intercept of the straight line interpolating data points should yield the value of K. However, the intercepts are both remarkably small, i.e. non distinguishable from zero within the experimental error. This result indicates that the K values are very high and the binding reaction is almost quantitative. It can thus be concluded that, despite the relatively high ionic strength of the medium that (in particular in the case of magnesium) should disfavour the binding of the positively charged coralyne to the negatively charged polynucleotide, the affinity of the intercalating dye to the tetra-aggregate is very high.

Conclusions

It was shown that magnesium and nickel can induce disproportion of poly(A)poly(U) to give a triple helix form. The process goes through an intermediate step where an aggregate is formed, whose simplest structure can be represented as a tetra-aggregate formed by two dye/double helix units. The tetra-aggregate evolves to give the triplex. However, in the presence of high metal ion content or by increasing the temperature, the last step does not occur and the aggregate remains the major species. The metal ion also stabilises the triplex, as confirmed by the increasing melting temperature of this form under different MgCl₂ concentration conditions. Further studies are needed to enlighten the exact structure of the tetra-aggregate. The collected data give information on a complex synergistic system where the action of an intercalating dye (coralyne), of metal ions (Na⁺, Mg²⁺ or Ni²⁺) and of temperature all concur in the stabilisation of a peculiar polymer form, duplex, triplex or four-strand aggregate. The efficiency of the investigated metal ions in promoting the transformation of AUD into UAUD changes in the order [Ni²⁺] >> [Mg²⁺] >> [Na⁺]. Coralyne strongly interacts also with the aggregate, in a way that does not significantly depend on the metal ion type or content.

Acknowledgements

Financial support by Obra Social La Caixa (OSLC-2012-007) is gratefully acknowledged.

REFERENCES

- [1] J. Choi, T. Majima, Conformational changes of non-B DNA, *Chem Soc Rev* 40 (2011) 5893-5909.
- [2] A. Rich, DNA Comes in Many Forms, *Gene* 135 (1993) 99-109.
- [3] M.L. Bochman, K. Paeschke, V.A. Zakian, DNA secondary structures: stability and function of structures., *Nat. Rev. Genet.* 13 (2012) 770-780.
- [4] M. Di Antonio, R. Rodriguez, S. Balasubramanian, Experimental approaches to identify cellular G-quadruplex structures and functions., *Methods (Amsterdam, Neth.)* 57 (2012) 84-92.
- [5] S. Buchini, C.J. Leumann, Recent improvements in antigene technology, *Curr Opin Chem Biol* 7 (2003) 717-726.

- [6] Q. Liu, A. Deiters, Optochemical Control of Deoxyoligonucleotide Function via a Nucleobase-Caging Approach., *Acc. Chem. Res.* 47 (2014) 45-55.
- [7] Z. Li, T.M. Rana, Therapeutic targeting of microRNAs: current status and future challenges., *Nat. Rev. Drug Discovery* 13 (2014) 622-638.
- [8] J.L. Huppert, S. Balasubramanian, G-quadruplexes in promoters throughout the human genome, *Nucleic Acids Res* 35 (2007) 406-413.
- [9] T.R. Cech, Beginning to understand the end of the chromosome, *Cell* 116 (2004) 273-279.
- [10] J. Muller, Functional metal ions in nucleic acids, *Metallomics* 2 (2010) 318-327.
- [11] F. Mocci, A. Laaksonen, Insight into nucleic acid counterion interactions from inside molecular dynamics simulations is "worth its salt", *Soft Matter* 8 (2012) 9268-9284.
- [12] N.V. Hud, A.E. Engelhart, Sequence-specific DNA-metal ion interactions, in: N.V. Hud (Eds.), RSC publishing, 2009, pp. 75-117.
- [13] R.K.O. Sigel, H. Sigel, A Stability Concept for Metal Ion Coordination to Single-Stranded Nucleic Acids and Affinities of Individual Sites, *Acc. Chem. Res.* 43 (2010) 974-984.
- [14] T. Biver, A. Boggioni, B. Garcia, J.M. Leal, R. Ruiz, F. Secco, M. Venturini, New aspects of the interaction of the antibiotic coralyne with RNA: coralyne induces triple helix formation in poly(rA)poly(rU), *Nucleic Acids Res* 38 (2010) 1697-1710.
- [15] H. Krakauer, Thermodynamic Analysis of Influence of Simple Mono- and Divalent-Cations on Conformational Transitions of Polynucleotide Complexes, *Biochemistry-U.S.* 13 (1974) 2579-2589.
- [16] V.A. Sorokin, V.A. Valeev, G.O. Gladchenko, M.V. Degtiar, Y.P. Blagoi, Ni²⁺ ion effect of conformations on single-, double and three-stranded homopolynucleotides containing adenine and uracil, *Macromol Biosci* 1 (2001) 191-203.
- [17] V.A. Sorokin, V.A. Valeev, G.O. Gladchenko, M.V. Degtiar, V.A. Karachevtsev, Y.P. Blagoi, Mg²⁺ ion effect on conformational equilibrium of polyA₂polyU and polyA₁polyU in aqueous solutions, *Int J Biol Macromol* 31 (2003) 223-233.
- [18] B. Garcia, S. Ibeas, R. Ruiz, J.M. Leal, T. Biver, A. Boggioni, F. Secco, M. Venturini, Solvent Effects on the Thermodynamics and Kinetics of Coralyne Self-Aggregation, *J Phys Chem B* 113 (2009) 188-196.
- [19] H. Diebler, F. Secco, M. Venturini, The Binding of Mg(II) and Ni(II) to Synthetic Polynucleotides, *Biophys Chem* 26 (1987) 193-205.
- [20] F.J. Hoyuelos, B. Garcia, J.M. Leal, N. Busto, T. Biver, F. Secco, M. Venturini, RNA triplex-to-duplex and duplex-to-triplex conversion induced by coralyne, *Phys Chem Chem Phys* 16 (2014) 6012-6018.
- [21] G. Strunk, H. Diebler, Binding of Divalent Metal-Ions to Synthetic Double-Stranded Polyribonucleotides, *J Chem Soc Dalton* (1994) 1929-1934.
- [22] D. Porschke, Thermodynamic and Kinetic-Parameters of Ion Condensation to Polynucleotides - Outer Sphere Complex Formed by Mg⁺⁺ Ions, *Biophys Chem* 4 (1976) 383-394.
- [23] B.I. Kankia, Mg²⁺-induced triplex formation of an equimolar mixture of poly(rA) and poly(rU), *Nucleic Acids Res* 31 (2003) 5101-5107.
- [24] M.T. Record, C.F. Anderson, T.M. Lohman, Thermodynamic Analysis of Ion Effects on Binding and Conformational Equilibria of Proteins and Nucleic-Acids - Roles of Ion Association or Release, Screening, and Ion Effects on Water Activity, *Q Rev Biophys* 11 (1978) 103-178.
- [25] T. Biver, F. Secco, M.R. Tine, M. Venturini, Kinetics and equilibria for the formation of a new DNA metal-intercalator: the cyclic polyamine Neotrien/copper(II) complex, *J Inorg Biochem* 98 (2004) 33-40.

Mg(II) and Ni(II) induce aggregation of poly(rA)poly(rU) to either tetra-aggregate or triplex depending on the metal ion concentration

Tarita Biver*, Natalia Busto, Begoña García, José Maria Leal, Luisa Menichetti, Fernando Secco, Marcella Venturini

Abstract

The ability of magnesium(II) and nickel(II) to induce dramatic conformational changes in the synthetic RNA, poly(a)poly(U), has been investigated. Kinetic experiments, spectrofluorometric titrations, melting experiments and DSC measurements contribute in shedding light on a complex behaviour where the action of metal ions (Na^+ , Mg^{2+} , Ni^{2+}), in synergism with other operators, as the intercalating dye coralyne and temperature, all concur in stabilizing a peculiar RNA form. Mg^{2+} and Ni^{2+} (M) bind rapidly and almost quantitatively to the duplex (AU) to give a RNA/metal ion complex (AUM). Then, by the union of two AUM units, an unstable tetra-aggregate ($\text{UAUA}(\text{M}_2)^*$) is formed which, in the presence of a relatively modest excess of metal, evolves to the UAUM triplex by releasing a single AM strand. On the other hand, under conditions of high metal content, the $\text{UAUA}(\text{M}_2)^*$ intermediate rearranges to give a more stable tetra-aggregate ($\text{UAUA}(\text{M}_2)$). As concerns the role of coralyne (D), it is found that D strongly interacts with $\text{UAUA}(\text{M}_2)$. Also, in the presence of coralyne, the ability of divalent ions to promote the transition of AUD into UAUD is enhanced, according to the efficiency sequence $[\text{Ni}^{2+}] \gg [\text{Mg}^{2+}] \gg [\text{Na}^+]$.

Keywords RNA, stabilisation, disproportion, non-canonical structure, quadruplex

Corresponding Author: Tarita Biver

Fax Number +390502219260, email tarita.biver@unipi.it

Introduction

It is now clear that non-canonical forms of polynucleotides, such as triple or quadruple helices, play a pivotal role in a wide number of biochemical reactions [1-4]. As concerns triplexes, their task in the “antigen” and/or “antisense” strategies is also a motif of major interest [5-7]. On the other hand, quadruple helices are envisaged to be present in the genome [8] and to constitute important regulators of both DNA and RNA polynucleotides [9]. The three-dimensional architecture of the above structures depends also on the presence metal ions. Given the negative charge of the phosphate-sugar backbone, positively charged counter-ions are crucial for stabilisation of complex structures [10, 11]. There is now substantial evidence that metal ions bind to specific sites [12, 13], stabilizing local motifs and positioning themselves correctly to aid (or even enable) a catalytic mechanism, as for instance in ribozymes. It should also be noted that the reverse effect has been observed, i.e. nucleic acids are able to catalyze reactions between metal ions [14, 15]. The effect exerted depends not only on the concentration but on the type of metal ion involved.

The formation of complex structures can also be induced by intercalating dyes: we have recently demonstrated that coralyne is able to induce triple helix formation in poly(rA)poly(rU), through an intermediate step that involves formation of a tetra-aggregate [15]. As regards the synthetic RNA poly(rA)poly(rU), literature data are limited to the thermodynamic aspects of duplex-triplex transitions induced by Mg^{2+} and Ni^{2+} ions at low concentration [16-18]. In the present work, we have analysed the kinetic aspects of the transitions induced by relatively high amounts of Mg^{2+} and Ni^{2+} in order to acquire information about the binding mechanism and the conditions that favour the stabilization of different RNA multiplexes. Moreover, the possible synergistic effects induced by the presence of coralyne and the binding of coralyne to the non-canonical forms are also investigated.

Materials and methods

Materials Ultra-pure water from a Millipore S.A. 670120 water purification system was used throughout. All reagents (Sodium Cacodylate, NaCl, $MgCl_2$, $NiCl_2$, Coralyne, poly(rA)poly(rU) and poly(rU) (lyophilised sodium salts)) were analytical grade from Sigma and were used as received. The stock solutions of the salts were obtained by dissolving appropriately weighted amounts in water. Poly(rA)poly(rU) and poly(rU) were dissolved into water. Their concentration was measured spectrophotometrically using the molar extinction coefficients (ϵ) obtained from the sample certificate: for poly(rA)poly(rU) $\epsilon = 14900 \text{ M}^{-1}\text{cm}^{-1}$ at 260 nm, pH = 7, I = 0.10 M (NaCl) and for poly(rU) $\epsilon = 8900 \text{ M}^{-1}\text{cm}^{-1}$ at 260 nm, pH = 7, I = 0.10 M (NaCl). The polynucleotide molar concentration is indicated as C_p . The working solutions were kept at 4°C and used within a week.

From now on poly(rA)poly(rU) will simply be denoted as poly(A)poly(U) or AU. Coralyne solutions were prepared by dissolving weighted amounts of the solid dye in MillyQ water (MW = 417.89). Both solid and solutions were kept in the dark at 4°C and used within two days; the molar concentration of the dye is indicated as C_D .

Methods . The pH measurements were done using a Metrohm pH-meter. All solutions were kept at pH = 7.0 using a 0.01M Sodium Cacodylate buffer ($\text{NaCac} = (\text{CH}_3)_2\text{AsO}_2\text{Na}$).

UV-vis spectrophotometry The kinetic measurements have been done using a Perkin-Elmer Lambda 35 double beam spectrophotometer with temperature control to within $\pm 0.1^\circ\text{C}$. The reaction was started upon addition of MgCl_2 (or NiCl_2) to solutions of poly(A)poly(U) and its rate was measured by monitoring the temporal variation of the absorbance at 260 nm. The dead time (interval between mixing and start of recording) is estimated to be as low as 5 s.

Spectrofluorometry Fluorescence measurements were performed using a Perkin Elmer LS55 spectrofluorometer with temperature control to within $\pm 0.1^\circ\text{C}$. In the coralyne/RNA spectrofluorometric titrations, increasing amounts of the polymer are added to the dye solution directly in the spectrofluorometric cell (both solutions being kept at the same pH and ionic strength values). The titrations of the poly(A)poly(U)/coralyne system with salts were performed by adding increasing amounts of the metal ion solution to a polymer solution present in the cell at a given poly(A)poly(U)/coralyne ratio. In another set of experiments, a coralyne solution containing a known concentration of NaCl, MgCl_2 or NiCl_2 , was titrated with poly(A)poly(U) containing the identical metal ion concentration. Note that the spectrofluorometric approach and the high fluorescence efficiency of coralyne enable very low concentration of the intercalating dye be used (10^{-7} M) so that problems originated by dye self-aggregation process could be avoided [19]. The additions were made using a Hamilton syringe connected to a micrometric screw that enabled volumes as small as 0.166 μL to be added.

Melting experiments The melting experiments were performed using a Hewlett-Packard 8452A (Agilent) single beam, diode array apparatus that was employed to monitor the absorbance variation with temperature at 260 nm using a scanning rate of $0.2^\circ\text{C}/\text{min}$ and 1 min stabilisation time for each step (1 cm optical path length). The temperature control was to within 0.01°C . The melting temperature T_m is obtained by the first derivative of the melting plot. In the experiments on poly(A)poly(U) at different metal ion content the polynucleotide concentration is kept at 1.7×10^{-5} M. The desired amount of MgCl_2 was added directly in the spectrophotometric cell containing the poly(A)poly(U) solution and the mixture was left to equilibrate for 2h. The experiments in the presence of coralyne were performed at constant dye concentration ($C_D = 1.7 \times 10^{-5}$ M) and the

polynucleotide concentration was appropriately varied to obtain the desired C_D/C_P ratio. The dye/polymer mixture was left to reach equilibrium for 2h before starting the melting experiment.

Circular Dichroism (CD) CD spectra (200 ÷ 700 nm, 1.0 cm path length) were registered using a MOS-450 Biologic (Claix, France) apparatus equipped with $\pm 0.1^\circ\text{C}$ temperature control. CD titrations were done by directly adding calibrated amounts of dye to the polymer solution already present in the cell.

Differential Scanning Calorimetry (DSC) Differential Scanning Calorimeter (DSC) data were obtained using a Setaram micro DSC III differential scanning calorimeter. The thermodynamic parameters for the denaturalisation of poly(A)poly(U) ($C_P = 2.5 \times 10^{-4}$ M) at different Mg^{2+} contents were measured. The volume of the solution was 850 μL and the scan rate $1^\circ\text{C}/\text{min}$. All solutions were degasified for 15 min with a TA instruments apparatus before filling the cell. Data were analysed using the NanoAnalyze 2.0 software.

Results – poly(A)poly(U)/metal ions

Kinetic study of the poly(A)poly(U)/magnesium system

To find the reaction order with respect to poly(A)poly(U) and magnesium, two different sets of experiments were done: (A) variation of the poly(A)poly(U) concentration, C_P , at constant $[\text{Mg}^{2+}]$, (B) variation of $[\text{Mg}^{2+}]$ at constant C_P . Note that the metal ion concentration has been widely changed (from 2×10^{-3} M to 0.2 M). Figure 1B shows a kinetic experiment carried out at $C_P = 1.8 \times 10^{-5}$ M and $[\text{Mg}^{2+}] = 1.2 \times 10^{-2}$ M. Two kinetic effects of different amplitude are clearly observed. The fastest of them, characterized by an absorbance decrease, prevails when $[\text{Mg}^{2+}] < 1.2 \times 10^{-2}$ M (Figure 1A), whereas the slowest, characterized by an absorbance increase, prevails for $[\text{Mg}^{2+}] > 5.5 \times 10^{-2}$ M (Figure 1C). The two effects were analysed separately, being well separated in the time scale.

Fast effect – Absorbance decrease The fast kinetic effect was analysed using the initial rate approach. The absorbance variation in time is evaluated by the slope of the initial portion of the curve. The initial slope ($\Delta\text{Abs}/\Delta t$) values were converted to variations of concentration in time using the molar extinction coefficient of poly(A)poly(U). The reaction order with respect to the polymer (experiments at constant $[\text{Mg}^{2+}]$ and different C_P) turned to be equal to one (Figure 2A, slope is 0.9 ± 0.1). Note that in this series of experiments the overall ionic strength is provided by the contribution of magnesium and is, therefore, constant. The determination of the reaction order respect to magnesium, instead, required experiments at different metal ion concentration (Figure 2B). Thus, a correction was applied to account for the dependence of the initial rate on the ionic strength of the medium (see Discussion).

Slow effect – Absorbance increase The kinetic experiments performed with $[\text{Mg}^{2+}]$ changing in the range $5.5 \times 10^{-2} \text{ M}$ - 0.2 M were also analysed using the initial rate method. Under these conditions (high metal ion content) the fast process occurs within the instrumental dead time and only the slow process could be observed (Figure 1C). The dilogarithmic graph shown in Figure 3A yields a slope of 1.8 ± 0.1 , corresponding to a reaction order of two with respect to RNA. Concerning experiments at constant C_P and different $[\text{Mg}^{2+}]$ (from 0.12 M to 0.61 M), the dilogarithmic plot (Figure 3B) is not strictly linear. This effect has been ascribed to the non constancy of the ionic strength which increases with the concentrations of Mg^{2+} ions. A correction for such an effect was therefore applied (see Discussion).

Kinetic study of the poly(A)poly(U)/nickel system

The poly(A)poly(U)/ Ni^{2+} system was analysed by the same method used for the poly(A)poly(U)/ Mg^{2+} system. Also in this case two distinct kinetic effects of opposite amplitude are observed upon addition of metal ion to the polynucleotide (Figure 1S-B of the Supporting Information). However, significantly lower metal ion concentrations (from $1.5 \times 10^{-3} \text{ M}$ to $1.5 \times 10^{-2} \text{ M}$) were needed to obtain effects of magnitude similar to that observed with magnesium. This result is in agreement with the higher efficacy of Ni^{2+} to affect the polynucleotide structure [20]. For $[\text{Ni}^{2+}] < 1.5 \times 10^{-3} \text{ M}$ the fast process is dominating (Figure 1S-A). The initial rate evaluation and relevant dilogarithmic plots (Figure 2S) yielded a reaction order equal to one with respect to poly(A)poly(U) and zero with respect to the metal ion. On the other hand, for $[\text{Ni}^{2+}] \geq 1.5 \times 10^{-3} \text{ M}$ the slow process is dominating (Figure 1S-C). Initial rate analysis and relevant dilogarithmic plots (Figure 3S) indicate that the reaction order with respect to polymer is two and with respect to nickel is zero. Note that in the case of nickel the ionic strength is so low that no ionic strength correction is needed.

Thermal denaturation experiments

Figure 4 shows the thermal denaturation profiles of the poly(A)poly(U)/ Mg^{2+} system for different magnesium contents. For $3.5 \times 10^{-3} \text{ M} \leq [\text{Mg}^{2+}] \leq 0.02 \text{ M}$, two distinct transitions could be observed. The amplitude and the melting temperature (T_m) of the first transition do increase as the metal ion concentration is raised, whereas the second transition ($T_m \approx 80^\circ\text{C}$) seems to be insensitive to $[\text{Mg}^{2+}]$. The melting profiles significantly change for $[\text{Mg}^{2+}] > 0.02 \text{ M}$ where the general trend is characterised by a dramatic decrease of the absorbance that reaches a minimum. After an initial slight absorbance increase a deep decrease of the signal occurs, the amplitude of the latter effect

being higher the higher the $[\text{Mg}^{2+}]$ concentration. Only for $T > 60^\circ\text{C}$, a biphasic trend, similar to that observed for $[\text{Mg}^{2+}] < 0.02 \text{ M}$ could be observed.

Circular Dichroism (CD) A circular dichroism titration was done by adding increasing amounts of MgCl_2 to a poly(A)poly(U) solution. The recorded CD spectra are shown in Figure 5A. The molar ellipticity in the UV region, typical of the polymer conformation, retains its band shape as $[\text{Mg}^{2+}]$ stays below 0.024 M but shows non negligible decrease for $[\text{Mg}^{2+}] \geq 0.053 \text{ M}$. Moreover, the maxima of the dichroic bands display a frequency shift as shown in Figure 5B with a minimum corresponding to about $[\text{Mg}^{2+}] = 0.11 \text{ M}$. This biphasic behaviour is in agreement with kinetic and thermal denaturation results.

Differential scanning calorimetry (DSC)

The effect of magnesium on the thermal stability of poly(A)poly(U) was qualitatively analysed by DSC. The relevant thermograms are shown in Figure 4S of the Supporting Information. A single endothermic transition is observed, indicating the occurrence of a strand denaturation process. The temperature of the transition is $86.1 \pm 0.2 \text{ }^\circ\text{C}$ independently of the $\text{Mg}(\text{II})$ content. Accordingly, the ΔH and ΔS values are also (within the experimental error) coincident at the different $[\text{Mg}^{2+}]$, being $\Delta H = 27 \pm 2 \text{ KJ}\cdot\text{mol}^{-1}$ and $\Delta S = 75 \pm 5 \text{ J}\cdot\text{mol}^{-1}\cdot\text{K}^{-1}$ ($[\text{NaCac}] = 0.01 \text{ M}$, $\text{pH} = 7.0$, $T = 25^\circ\text{C}$). These values are in agreement with previous evaluations [21].

Results – poly(A)poly(U)/coralyne/metal ions

It has already been shown that coralyne (Figure 6) interacts with poly(A)poly(U) in a complex way where triple helix formation is induced [15, 22]. In the present study we have investigated the influence of metal ions on the poly(A)poly(U)/coralyne system and the ability of coralyne to interact with the poly(A)poly(U)/metal ion system.

Spectrofluorometric titrations Spectrofluorometric titrations of coralyne with poly(A)poly(U) were done in aqueous solutions containing different concentrations of NaCl ranging between 0.020 M to 1.0 M (Figure 5S). The binding isotherms are biphasic independently of the salt content: a fluorescence decrease is displayed in the first phase whereas the second phase is related to a fluorescence increase. On the other hand, the slope of the branches and the minimum of the binding isotherm (i.e. the position of the slope inversion) both depend on the added salt content. Then a different experiment was performed as follows: a mixture of poly(A)poly(U) and coralyne was prepared with C_P/C_D equal to the minimum of the binding isotherm ($C_D/C_P = 0.23$, $C_D = 6.5 \times 10^{-7}$, Figure 5S). Then the mixture was titrated with NaCl and an increase of fluorescence was observed

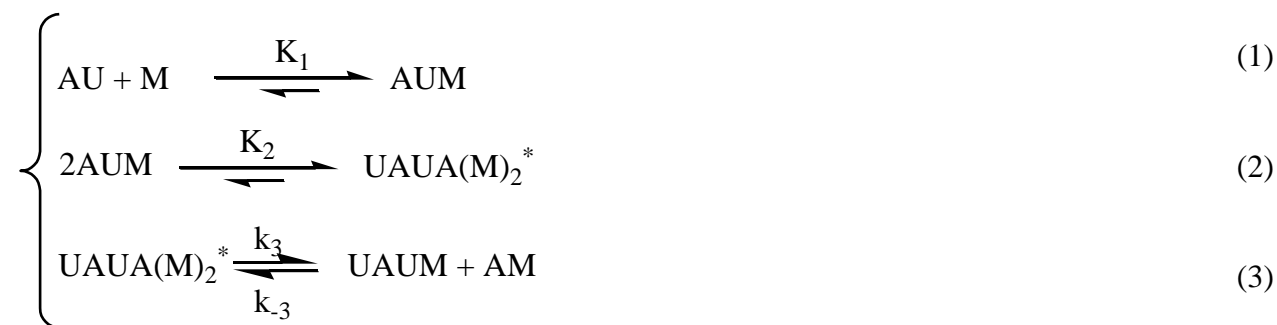
(Figure 7A). The experiment was repeated with the same starting mixture but using MgCl₂ or NiCl₂ as titrating agents in place of NaCl. The observed fluorescence increase is qualitatively the same, but lower amounts of MgCl₂ (Figure 7B) and much lower of NiCl₂ (Figure 7C) are needed to complete the titration.

Finally, a further experiment was devised as follows: a mixture of poly(A)poly(U) and MgCl₂ was incubated at 25C° for 1h. The mixture was then titrated with coralyne. Note that MgCl₂ was present in the coralyne solution at the same concentration as in the RNA. The magnesium level was 0.3M in both solutions i.e. higher than that employed in the experiment of Figure 1C. Therefore, in this experiment, we analysed the binding of the coralyne to the peculiar polymer conformation induced by high metal ion content. The resulting binding isotherm is shown in Figure 8A. Figure 8B shows the analogous experiment, where MgCl₂ 0.3M is replaced by NiCl₂ 0.048M. The trends found in both cases reveal the occurrence of strong binding of coralyne dye to the polymer/metal ion systems.

Discussion

Poly(A)poly(U)/Mg²⁺ and Poly(A)poly(U)/Ni²⁺

On the basis of the results of the kinetic and melting studies the following reaction scheme (equations 1-3) is proposed to represent the time course of the first kinetic phase shown in Figure 1A.



It should be noticed that the amplitudes of the fast phase were found to decrease as [M] is increased (Figure 6S), meaning that sequence (1)-(3) represents an equilibrium process. Here, M is the divalent metal ion (Mg²⁺ or Ni²⁺) and AUM a poly(A)poly(U)/metal ion complex [19]. The equilibrium constant of reaction (1) is known from the literature and is relatively high ($K_1 \approx 8 \times 10^3$ for magnesium in [Na⁺] = 0.01M [23]). Therefore, in the presence of relatively high amounts of metal ion, reaction (1) can be supposed to be shifted towards the AUM complex. Moreover, reaction (1) is so fast [24] that AUM should be considered as already formed at the start of the spectrophotometric experiments. Reaction (2) gives rise to the tetra-aggregate UAUA(M₂)* where

two AUM strands are held together by electrostatic Mg^{2+} (or Ni^{2+} bridges). In the presence of relatively low amounts of divalent metal ions a triplex, UAUM, is formed according to reaction (3). This transformation is possible as the aggregated species $UAUA(M_2)^*$ is unstable and can easily expel a metal bound poly(A) single strand (AUM). This hypothesis agrees with the finding that low magnesium contents can stabilise the poly(U)poly(A)poly(U) triple helix [18].

On the basis of reaction scheme (1-3) it can be demonstrated (see the Supporting Information) that the initial rate V_0 is given by the relationship $V_0 = k_3 C_P / 2$. This equation indicates that the reaction order with respect to the polymer is one, in agreement with experiment. On the other hand, the experiments performed to find the order of reaction with respect to magnesium, show that the rate dependence on the metal ion concentration is positive (slope in Figure 2B is 0.6 ± 0.1) but less than first-order. We ascribe the slightly increasing trend to an ionic strength effect. Actually, being reaction (1) very fast and almost quantitative and reaction (3) insensitive to the salt content, reaction (2) will dominate the electrostatic behaviour. The electrostatic theory dictates that this reaction should display a rate enhancement on increasing the metal ion concentration because the two AUM molecules bear the same charge. Correction for the electrostatic contribution (using the Debye-Hückel limiting law or Guggenheim equation [24]) reduces the slope of the plot of Figure 2B thus bringing the order of reaction with respect to magnesium near to zero, in agreement with the rate equation derived by the proposed reaction scheme.

In the presence of high amounts of metal ions, reaction (3) is replaced by reaction (4), which corresponds to the rate-determining conversion of the unstable species $UAUA(M_2)^*$ to the more stable tetra aggregate $UAUA(M)_2$. The hypothesis of the formation of an aggregate is in agreement with previous observations that suggest the divalent ions (and in particular magnesium) are able to strengthen inter-strand interactions in poly(A) [21]. It has also been demonstrated that an increase of the Mg^{2+} concentration in poly(A)/ Mg^{2+} mixtures induces aggregation/condensation processes of the single strand that results in absorbance increases [21].



Reaction (4) represents an equilibrium because the analysis of the dependence of the overall rate constant on the polymer concentration yields a straight line with a positive intercept (Figure 7S) which indicates the occurrence of the reverse step.

The kinetic equation for the (1)-(2)-(4) system is (see Supporting Information) is the following

$$V_0 = k_2'K_2 \frac{C_p^2 K_1^2 [M]^2}{(1 + K_1^2 [M]^2 + 2K_1 [M])} \quad (5)$$

Being under the experimental conditions $K_1^2 [M]^2 \gg 1 + 2K_1 [M]$, it results that $V_0 = k_2'K_2 C_p^2$. The reaction order is therefore two with respect to polymer and zero with respect to metal ion, in agreement with experimental findings. Also in this case correction for the electrostatic salt effect has been applied to find the order of reaction respect to magnesium.

The proposed mechanism is corroborated by the analysis of the melting profiles. Actually the occurrence of two transitions, observed at low magnesium content (Figure 4) demonstrates the presence of a triple helix as a major component at 25°C. In the first transition the triplex poly(U)poly(A)poly(U) converts to the duplex by releasing a poly(U) single strand. The amplitude and melting temperature for this step depends on the Mg^{2+} concentration: it is higher the higher the metal content until $[Mg^{2+}] \approx 0.02M$, in agreement with an increased stabilisation of the triplex. The second transition corresponds to dissociation to give poly(A) and poly(U) single strands and is insensitive to the presence of Mg^{2+} ions (ca. 80 °C at every $[MgCl_2]$ employed). This finding indicates weak interaction of the duplex with the metal ion at this temperature.

The change of the melting profiles at higher magnesium concentrations is in agreement with the presence of an aggregate. The higher initial absorbance value reveals that, for $[Mg^{2+}] = 0.025 M$ non-negligible amounts of $UAUA(M)_2$ are formed already at 20°C but its maximum extent occurs at 45°C. An increase of $[Mg^{2+}]$ results in a shift of the maximum aggregation toward lower temperatures. Actually, aggregation is favoured by this metal ion to such a level that, for $[Mg^{2+}] = 0.11 M$, the aggregate is the prevailing form already at 20°C. Similar behaviour has been observed for poly(A)/ Mg^{2+} where the increase of temperature favours single strands condensation [21]. Once the aggregate formed, a further temperature increase will produce the disproportion of the aggregate form into UAU triplex and U single strand. Under these conditions the absorbance reaches a minimum, as observed both in melting and in kinetic experiments. This process occurs also at lower temperatures for higher metal ion contents. After this stage, the trend will follow the typical biphasic trend of a triple helix, with total dissociation occurring again around 80°C. The here observed value of T_m (80°C) corresponds to the denaturation of the triplex in the absence of salts [15].

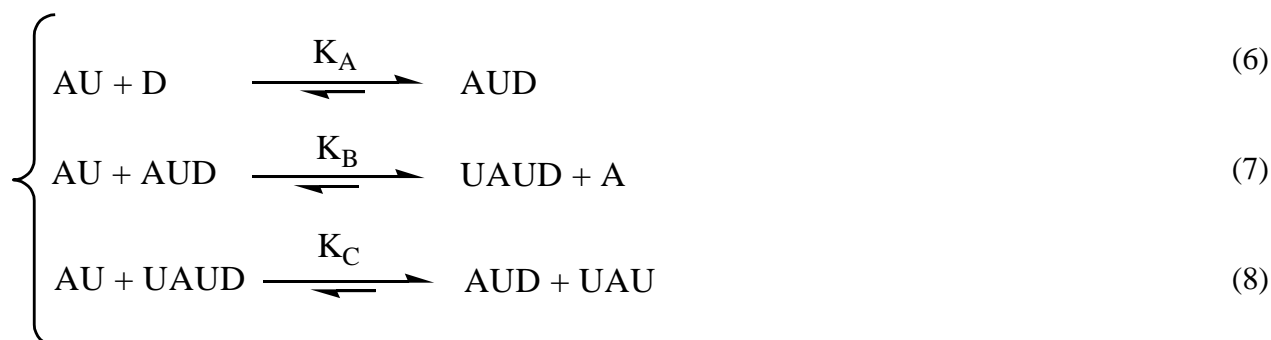
CD results confirm a picture where the metal ion content shifts the equilibria towards different RNA forms. For $[Mg^{2+}] < 0.01 M$ the triplex is majority, whereas increasing amounts of the metal ion stabilise a more aggregated form (devised here as the tetra-aggregate). The transitions duplex –

triplex – tetra-aggregate are accompanied by a loss of ellipticity that is negligible in the case of duplex – triplex transition, whereas is much more significant in the case of the step leading to the formation of the aggregate (Figure 5).

The DSC experiments show a single transition. The almost constant ΔH value found for different values of $[\text{MgCl}_2]$ confirms that in all cases the same transition is observed. This is likely the more energetic one and, being its ΔH value positive, it should represent the duplex to single strand transition. This result suggests that the other transitions (triplex-duplex and aggregate-triplex) are characterised by a lower enthalpic content. Note that, concerning the here investigated system, the DSC approach is scarcely suitable to put into evidence the details of the system behaviour. The reason of this fact can be found in the low sensitivity of the DSC method. Actually, if C_P concentrations similar to that of melting experiments ($C_P = 1.7 \times 10^{-5} \text{ M}$) would had been employed, the amplitude of the DSC graphs would had been 15 times lower respect to that of the experiment reported in Figure 4S and the experiments under these conditions would had been affected by high noise and error.

Poly(A)poly(U)/coralyne/metal ions

The spectrofluorometric titrations of the poly(A)poly(U)/coralyne/metal ions system (Figure 8S) were analyzed using equation (9), which was derived on the basis of the reaction mechanism written below [14].



In this mechanism the interaction between poly(A)poly(U) (AU) and coralyne (D) produces first the formation of the AUD complex which, in the second step, reacts with AU to produce a coralyne bound triplex (UAUD); in the final step D is rapidly exchanged between AU and UAU. The values of the equilibrium constants K_A , K_B and K_C , measured at different values of $[\text{NaCl}]$ are collected in Table 1S of the Supporting Information.

$$\frac{F}{C_D} = \phi_D + \frac{\Delta\phi_A K_A [AU] + \Delta\phi_B [AU] \sqrt{K_A K_B / ([D] + K_C / K_A)}}{1 + K_A [AU] + [AU] \sqrt{K_A K_B / ([D] + K_C / K_A)}} \quad (9)$$

In equation (9) $\Delta\phi_A = (\phi_{AUD} - \phi_D)$ and $\Delta\phi_B = (\phi_{UAUD} - \phi_D)$, whereas ϕ_i is the optical parameter of the i^{th} reactant. The decrease of fluorescence displayed by the binding isotherms (Figure 8S) corresponds to formation of AUD, whereas the subsequent fluorescence increase is related to the reactions (7) and (8).

The results have shown that the addition of metal ions to the poly(A)poly(U)/coralyne system strongly affects the thermodynamics of the system itself. The dependence of step (6) on the concentration of NaCl has been analyzed in terms of the Record theory [25] which requires that $\text{Log}K_A$ should depend linearly on $\text{Log}[\text{Na}^+]$ with a slope that corresponds to the number of Na^+ ions displaced from the polynucleotide upon binding of a dye molecule. The Record slope, for the present system, is equal to ca. 0.5, indicating that two molecules of coralyne are needed to displace one sodium ion.

Metal ions also affect the shape of the binding isotherm. Actually, the addition of NaCl to a mixture of poly(A)poly(U) and coralyne at C_P/C_D equal to the minimum of the binding isotherm shown in Figure 8S (where AUD is majority) produces a fluorescence increase. This finding reveals that sodium ions favour the formation of the triplex UAUD (which is more fluorescent than duplex) according to step (7). Reaction (10) could also be possible as an alternative to reaction (7), but the latter will prevail under conditions of polymer excess.



Sodium, magnesium and nickel ions show different ability to drive the system towards triplex formation (Figure 6).

The titrations of coralyne with solutions of poly(A)poly(U) containing a large metal ion amount of tetra-aggregate (Figure 7) have provided the binding affinity of coralyne to the $\text{UAUA}(\text{M})_2$ aggregate. The titrations have been quantitatively analysed using equation (11).

$$\frac{C_D C_P}{\Delta F} + \frac{\Delta F}{\Delta\phi^2} = \frac{1}{K\Delta\phi} + \frac{(C_P + C_D)}{\Delta\phi} \quad (11)$$

where K is the equilibrium constant for the binding of the dye (D) to the aggregate $\text{UAUA}(\text{M})_2$, (denoted as P) to give the $\text{DUAUA}(\text{M})_2$ complex (denoted as PD). $\Delta F = F - \phi_D C_D$, $\Delta\phi = \phi_{PD} - \phi_D$

and the $\Delta F/\Delta\phi^2$ term is not initially known but can be calculated using an iterative procedure [26]. The relevant plots are shown in Figure 6S; the ratio between slope and intercept of the straight line interpolating data points should yield the value of K. However, the intercepts are both remarkably small, i.e. non distinguishable from zero within the experimental error. This result indicates that the K values are very high and the binding reaction is almost quantitative. It can thus be concluded that, despite the relatively high ionic strength of the medium that should (in particular in the case of magnesium) disfavour the binding of the positively charged coralyne to the negatively charged polynucleotide, the affinity of the intercalating dye to the tetra-aggregate is very high.

Conclusions

It was shown that magnesium and nickel can induce disproportion of poly(A)poly(U) to give a triplex. The process involves an aggregated species, whose simplest structure can be that of a tetra-aggregate formed by two double helix units held together by metal ion bridges. At low salt content the tetra-aggregate is unstable and evolves towards the triplex but, increasing the metal ion content or the temperature, the last step is repressed and the tetra-aggregate undergoes stabilization. Tuning of triplex/tetra-aggregate predominance by calibrating the presence of suitable metal ions is confirmed by melting experiments carried changing the concentration of added MgCl₂. However, further studies are needed to enlighten the exact structure of the tetra-aggregate. The experiments in the presence of coralyne envisage a complex synergistic system where the action of the intercalating dye, the metal ions (Na⁺, Mg²⁺ or Ni²⁺) and temperature all concur in the stabilisation of a peculiar form of the polymer: duplex, triplex or four-strand aggregate. The efficiency of the investigated metal ions in promoting the duplex to triplex transformation changes in the order [Ni²⁺] >> [Mg²⁺] >> [Na⁺]. Coralyne strongly interacts also with the aggregate, in a way that does not significantly depend on the metal ion type or content.

List of abbreviations

AU	poly(rA)poly(rU) duplex
A	poly(rA) single strand
UAU	poly(rU)poly(rA)poly(rU) triplex
M	metal ion
AUM	metal ion/poly(rA)poly(rU) duplex complex
AM	metal ion/poly(rA) single strand complex
UAUA(M ₂)*	unstable metal ion/tetra-aggregate complex

UAUM	metal ion/poly(rU)poly(rA)poly(rU) triplex complex
UAUA(M ₂)	stable metal ion/tetra-aggregate complex
D	coralyne dye
AUD	coralyne/poly(rA)poly(rU) duplex complex
UAUD	coralyne/poly(rU)poly(rA)poly(rU) triplex complex
CD	Circular Dichroism
DSC	Differential Scanning Calorimetry

Acknowledgements

Financial support by Obra Social La Caixa (OSLC-2012-007) is gratefully acknowledged.

REFERENCES

- [1] J. Choi, T. Majima, Conformational changes of non-B DNA, *Chem. Soc. Rev.* 40 (2011) 5893-5909.
- [2] A. Rich, DNA Comes in Many Forms, *Gene* 135 (1993) 99-109.
- [3] M.L. Bochman, K. Paeschke, V.A. Zakian, DNA secondary structures: stability and function of structures., *Nat. Rev. Genet.* 13 (2012) 770-780.
- [4] M. Di Antonio, R. Rodriguez, S. Balasubramanian, Experimental approaches to identify cellular G-quadruplex structures and functions., *Methods* 57 (2012) 84-92.
- [5] S. Buchini, C.J. Leumann, Recent improvements in antigene technology, *Curr. Opin. Chem. Biol.* 7 (2003) 717-726.
- [6] Q. Liu, A. Deiters, Optochemical Control of Deoxyoligonucleotide Function via a Nucleobase-Caging Approach., *Acc. Chem. Res.* 47 (2014) 45-55.
- [7] Z. Li, T.M. Rana, Therapeutic targeting of microRNAs: current status and future challenges., *Nat. Rev. Drug Discovery* 13 (2014) 622-638.
- [8] J.L. Huppert, S. Balasubramanian, G-quadruplexes in promoters throughout the human genome, *Nucleic Acids Res.* 35 (2007) 406-413.
- [9] T.R. Cech, Beginning to understand the end of the chromosome, *Cell* 116 (2004) 273-279.
- [10] J. Muller, Functional metal ions in nucleic acids, *Metallomics* 2 (2010) 318-327.
- [11] F. Mocci, A. Laaksonen, Insight into nucleic acid counterion interactions from inside molecular dynamics simulations is "worth its salt", *Soft Matter* 8 (2012) 9268-9284.
- [12] N.V. Hud, A.E. Engelhart, Sequence-specific DNA-metal ion interactions, in: N.V. Hud (Eds.), RSC publishing, 2009, pp. 75-117.
- [13] R.K.O. Sigel, H. Sigel, A Stability Concept for Metal Ion Coordination to Single-Stranded Nucleic Acids and Affinities of Individual Sites, *Acc. Chem. Res.* 43 (2010) 974-984.
- [14] F. Secco, M. Venturini, M. Lopez, P. Perez, R. Prado, F. Sanchez, Effect of DNA on the rate of electron transfer reactions between non-intercalated reactants: kinetic study of the reactions $[\text{Ru}(\text{NH}_3)_5\text{pz}](2+)+[\text{Co}(\text{C}_2\text{O}_4)_3](3-)$ and $[\text{Ru}(\text{NH}_3)_5\text{py}](2+)+[\text{Co}(\text{NH}_3)_4\text{pzCO}(2)](2+)$ in aqueous solutions in the presence of DNA, *Phys. Chem. Chem. Phys.* 3 (2001) 4412-4417.
- [15] T. Biver, A. Boggioni, B. Garcia, J.M. Leal, R. Ruiz, F. Secco, M. Venturini, New aspects of the interaction of the antibiotic coralyne with RNA: coralyne induces triple helix formation in poly(rA)poly(rU), *Nucleic Acids Res.* 38 (2010) 1697-1710.
- [16] H. Krakauer, Thermodynamic Analysis of Influence of Simple Mono- and Divalent-Cations on Conformational Transitions of Polynucleotide Complexes, *Biochemistry* 13 (1974) 2579-2589.
- [17] V.A. Sorokin, V.A. Valeev, G.O. Gladchenko, M.V. Degtiar, Y.P. Blagoi, Ni²⁺ ion effect of conformations on single-, double and three-stranded homopolynucleotides containing adenine and uracil, *Macromol. Biosci.* 1 (2001) 191-203.
- [18] V.A. Sorokin, V.A. Valeev, G.O. Gladchenko, M.V. Degtiar, V.A. Karachevtsev, Y.P. Blagoi, Mg²⁺ ion effect on conformational equilibrium of polyA₂polyU and polyA₁polyU in aqueous solutions, *Int. J. Biol. Macromol.* 31 (2003) 223-233.
- [19] B. Garcia, S. Ibeas, R. Ruiz, J.M. Leal, T. Biver, A. Boggioni, F. Secco, M. Venturini, Solvent Effects on the Thermodynamics and Kinetics of Coralyne Self-Aggregation, *J. Phys. Chem. B* 113 (2009) 188-196.
- [20] H. Diebler, F. Secco, M. Venturini, The Binding of Mg(II) and Ni(II) to Synthetic Polynucleotides, *Biophys. Chem.* 26 (1987) 193-205.
- [21] B.I. Kankia, Mg²⁺-induced triplex formation of an equimolar mixture of poly(rA) and poly(rU), *Nucleic Acids Res.* 31 (2003) 5101-5107.
- [22] F.J. Hoyuelos, B. Garcia, J.M. Leal, N. Busto, T. Biver, F. Secco, M. Venturini, RNA triplex-to-duplex and duplex-to-triplex conversion induced by coralyne, *Phys. Chem. Chem. Phys.* 16 (2014) 6012-6018.

- [23] G. Strunk, H. Diebler, Binding of Divalent Metal-Ions to Synthetic Double-Stranded Polyribonucleotides, *J. Chem. Soc. Dalton* (1994) 1929-1934.
- [24] D. Porschke, Thermodynamic and Kinetic-Parameters of Ion Condensation to Polynucleotides - Outer Sphere Complex Formed by Mg^{++} Ions, *Biophys. Chem.* 4 (1976) 383-394.
- [25] M.T. Record, C.F. Anderson, T.M. Lohman, Thermodynamic Analysis of Ion Effects on Binding and Conformational Equilibria of Proteins and Nucleic-Acids - Roles of Ion Association or Release, Screening, and Ion Effects on Water Activity, *Q. Rev. Biophys.* 11 (1978) 103-178.
- [26] T. Biver, F. Secco, M.R. Tine, M. Venturini, Kinetics and equilibria for the formation of a new DNA metal-intercalator: the cyclic polyamine Neotrien/copper(II) complex, *J. Inorg. Biochem.* 98 (2004) 33-40.

Figure Legends

Figure 1. Kinetic curves for the poly(A)poly(U)/Mg²⁺ system; C_P = 1.8×10⁻⁵ M, [NaCac] = 0.01 M, pH = 7.0, λ = 260 nm, T = 25 °C. (A) [Mg²⁺] = 6.7×10⁻³ M, (B) [Mg²⁺] = 1.2×10⁻² M, (C) [Mg²⁺] = 0.2 M.

Figure 2. Fast effect for the poly(A)poly(U)/Mg²⁺ system, [NaCac] = 0.01 M, pH = 7.0, T = 25°C: dilogarithmic plot of initial rate (V₀) dependence on: (A) the polymer concentration C_P at [Mg²⁺] = 6.7×10⁻³ M, (B) the magnesium concentration at C_P = 1.8×10⁻⁵ M.

Figure 3. Slow effect for the poly(A)poly(U)/Mg²⁺ system, [NaCac] = 0.01 M, pH = 7.0, T = 25°C: dilogarithmic plot showing the initial rate (V₀) dependence on: (A) the polymer concentration C_P at [Mg²⁺] = 0.138 M, (B) on the magnesium concentration at C_P = 1.8×10⁻⁵ M.

Figure 4. Melting profiles for the poly(A)poly(U)/Mg²⁺ system at different magnesium content; C_P = 1.7×10⁻⁵ M, [NaCac] = 0.01 M, pH = 7.0, λ = 260 nm.

Figure 5. CD titration of poly(A)poly(U) with MgCl₂; C_P = 1.5×10⁻⁵ M, pH = 7.0, 25°C. (A) CD curves when [MgCl₂] increases from 0 M to 0.5 M as indicated by the arrow: (a) 0 M, (b) 1.2×10⁻³ M, (c) 2.4×10⁻³ M, (d) 4.8×10⁻³ M, (e) 9.5×10⁻³ M, (f) 0.024 M, (g) 0.053 M, (h) 0.11 M. (B) Position of the maximum of the positive dichroic band as a function of the magnesium content (line to drive the eye).

Figure 6. Coralyne chloride (8-methyl-2,3,10,11-tetramethoxydibenzo[a,g]quinolizinium chloride) molecular formula.

Figure 7. Trends showing fluorescence increase when increasing amounts of metal ions are added to a poly(A)poly(U)/coralyne mixture (C_P/C_D chosen to ensure maximum formation of the polymer/dye complex); C_D = 6.5×10⁻⁷ M, C_P = 2.8×10⁻⁵ M, pH = 7.0, T = 25°C, λ_{exc} = 420 nm, λ_{em} = 470 nm; (A) [Na⁺], (B) [Mg²⁺], (C) [Ni²⁺].

Figure 8. Binding isotherm for the poly(A)poly(U)/coralyne system (A) in MgCl₂ 0.3M, (B) in NiCl₂ 0.048M; C_D = 6.5×10⁻⁷ M, pH = 7.0, T = 25°C, λ_{exc} = 420 nm, λ_{em} = 470 nm.

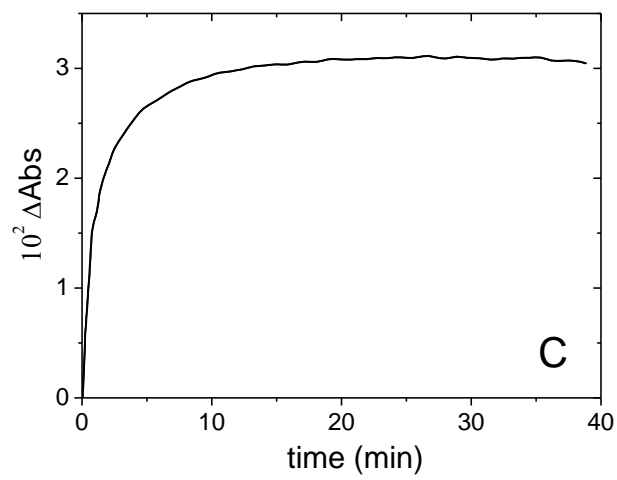
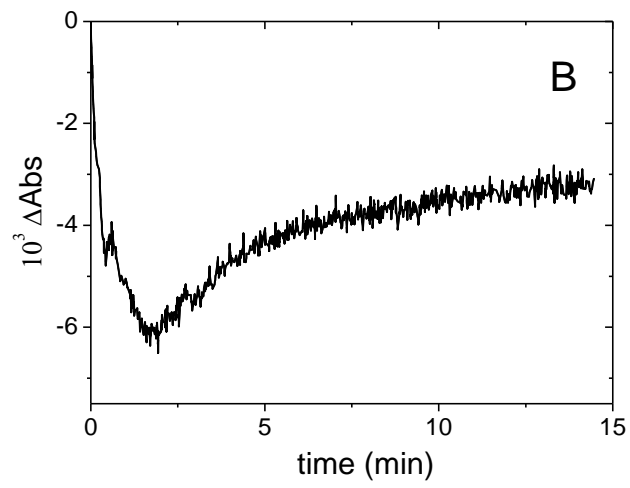
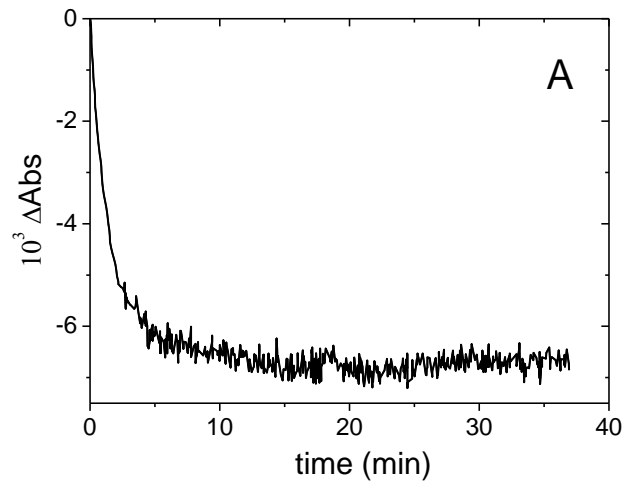


FIGURE 1

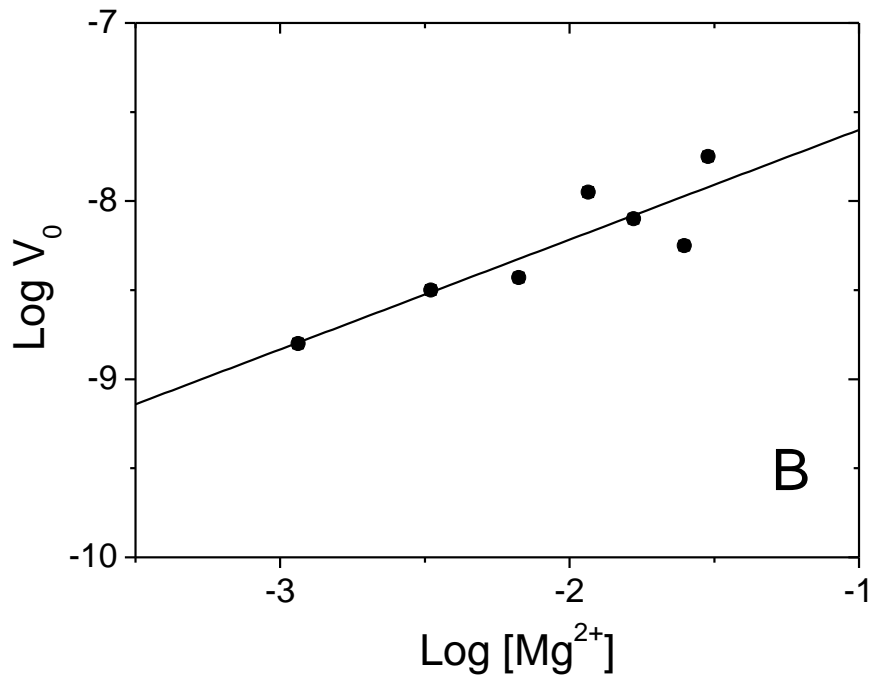
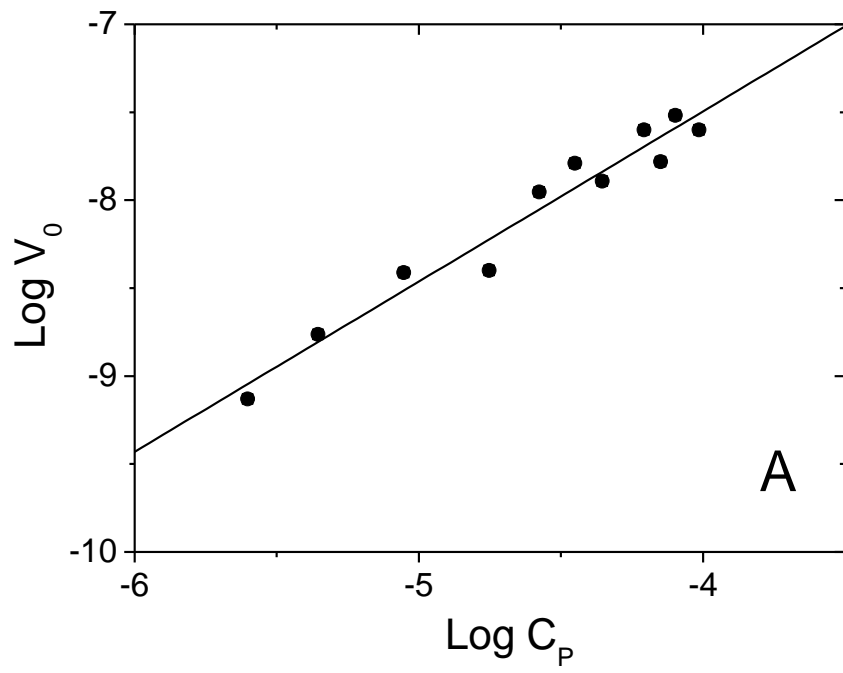


FIGURE 2

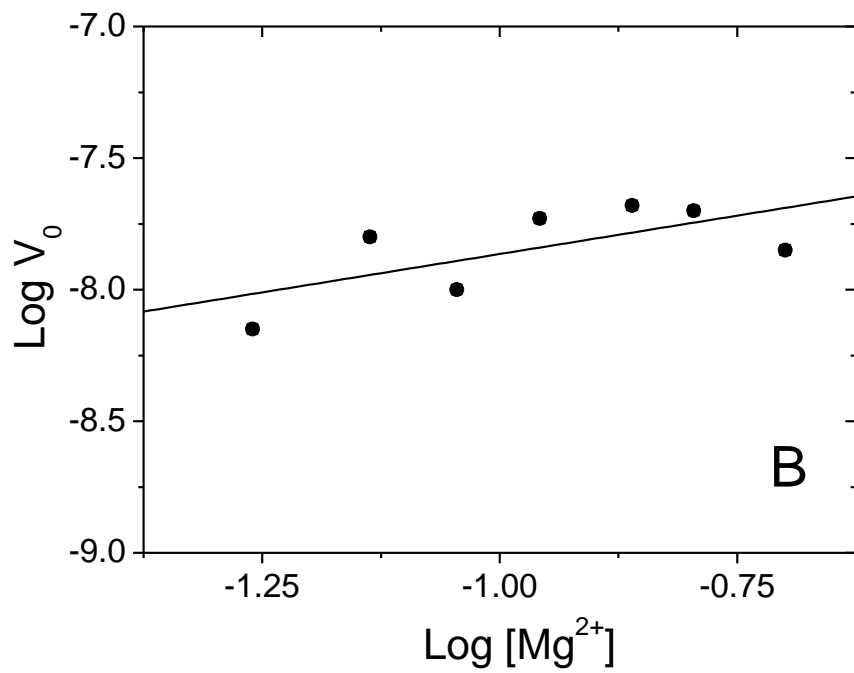
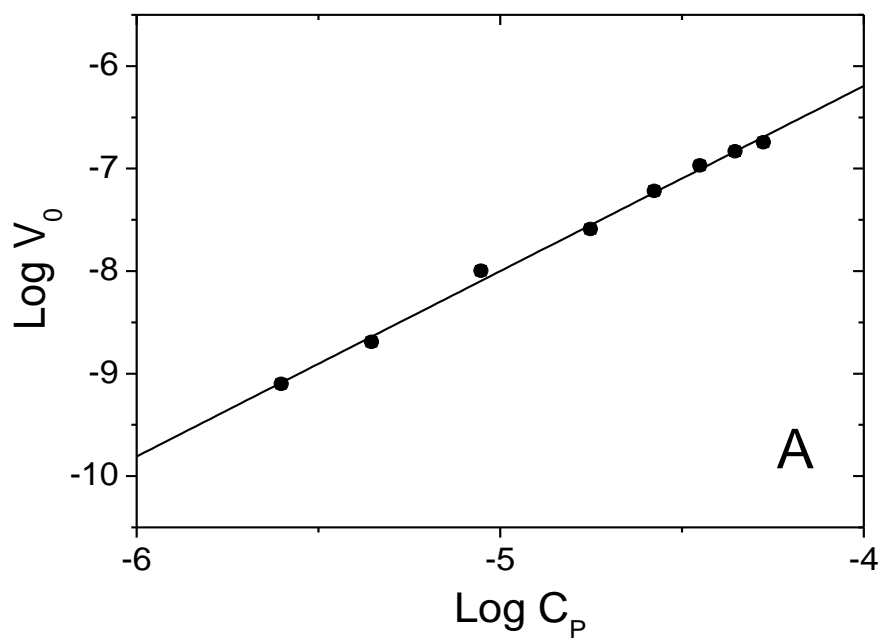


FIGURE 3

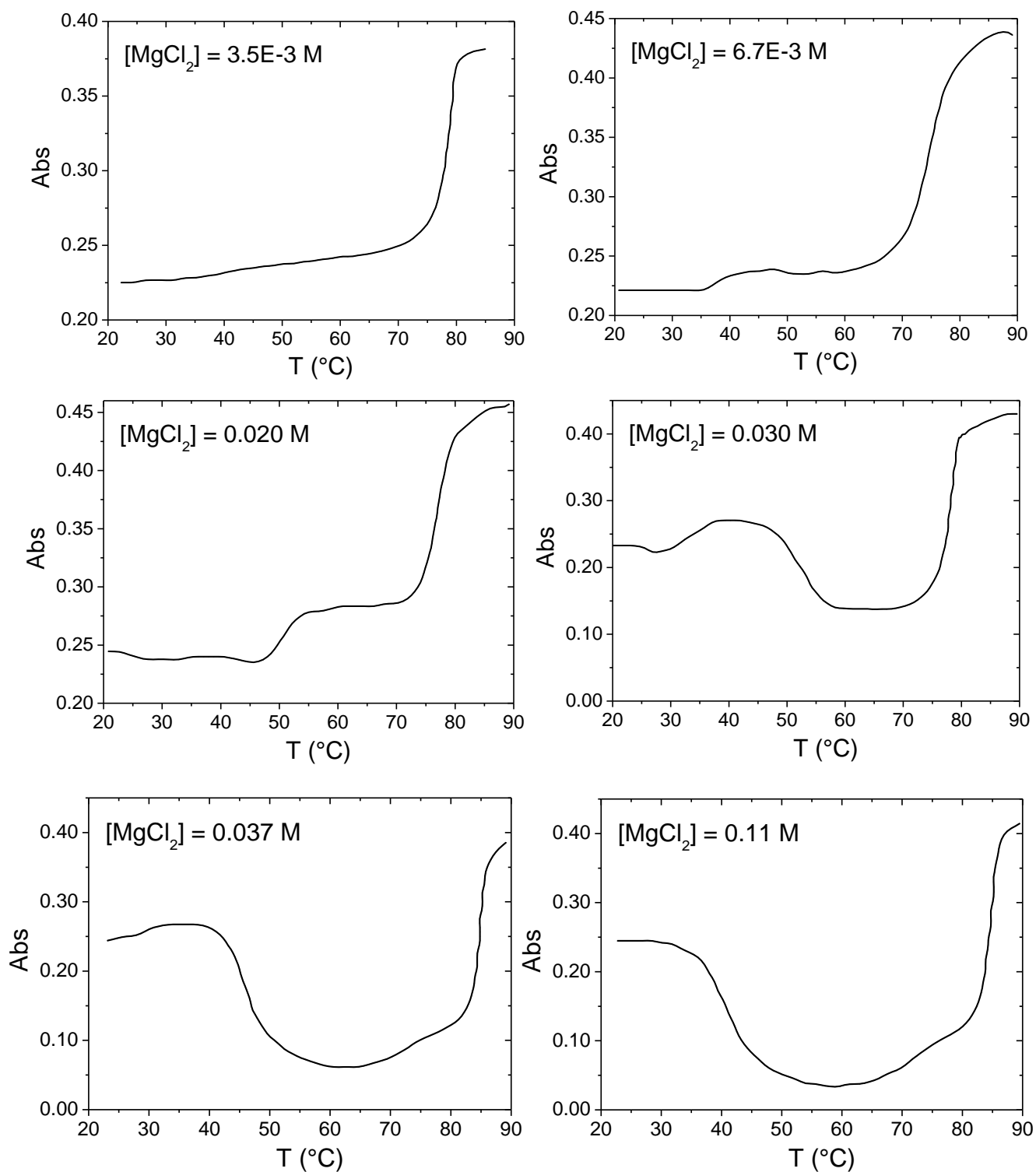


FIGURE 4

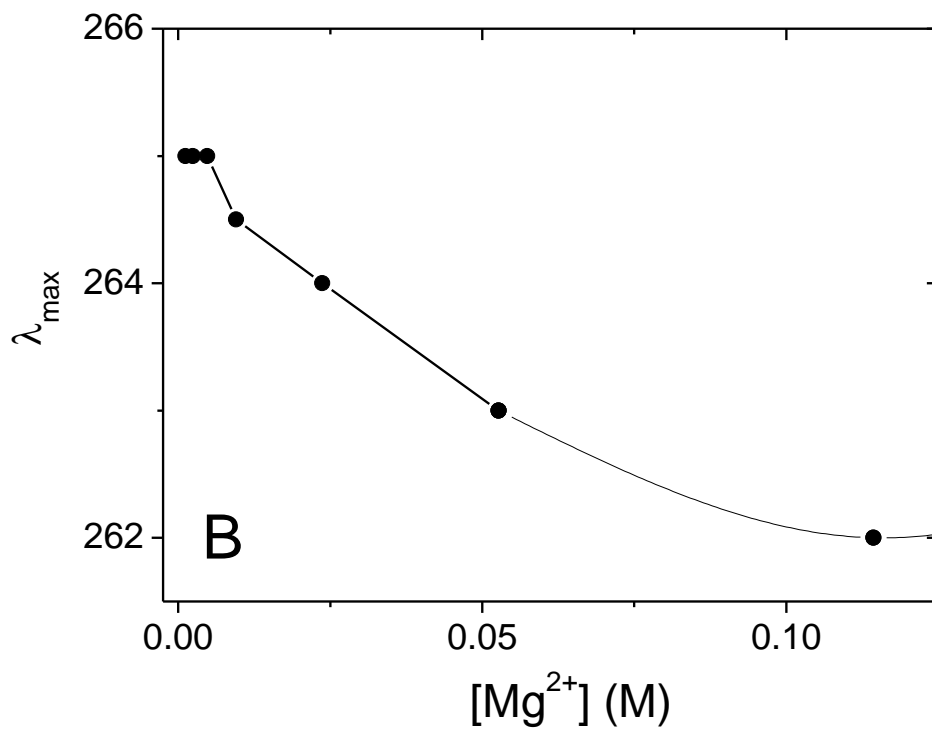
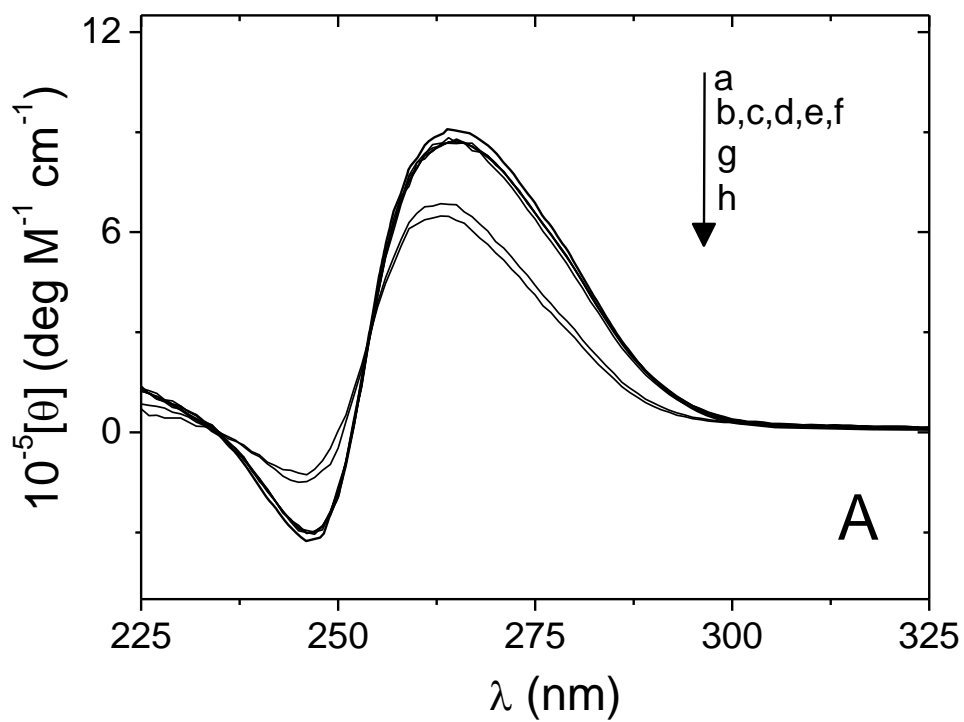


FIGURE 5

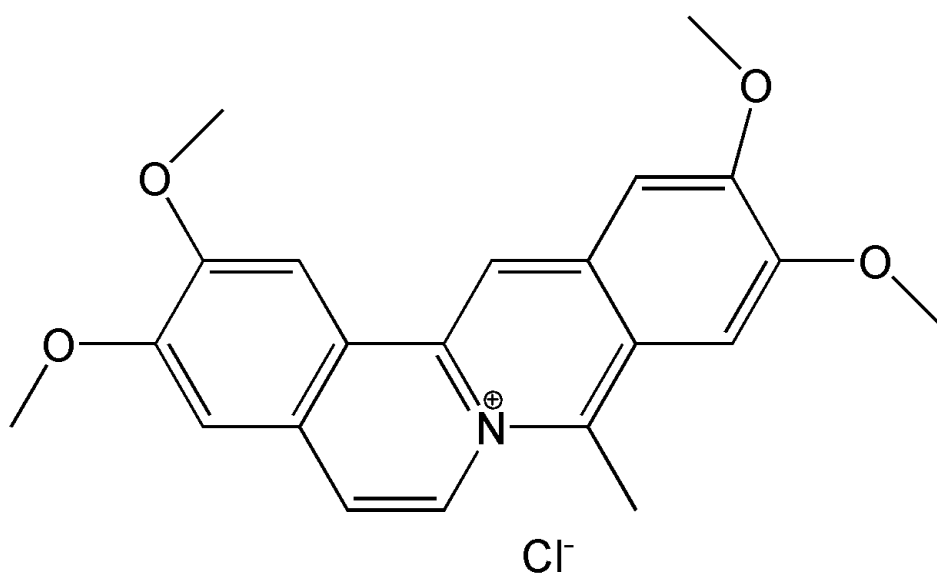


FIGURE 6

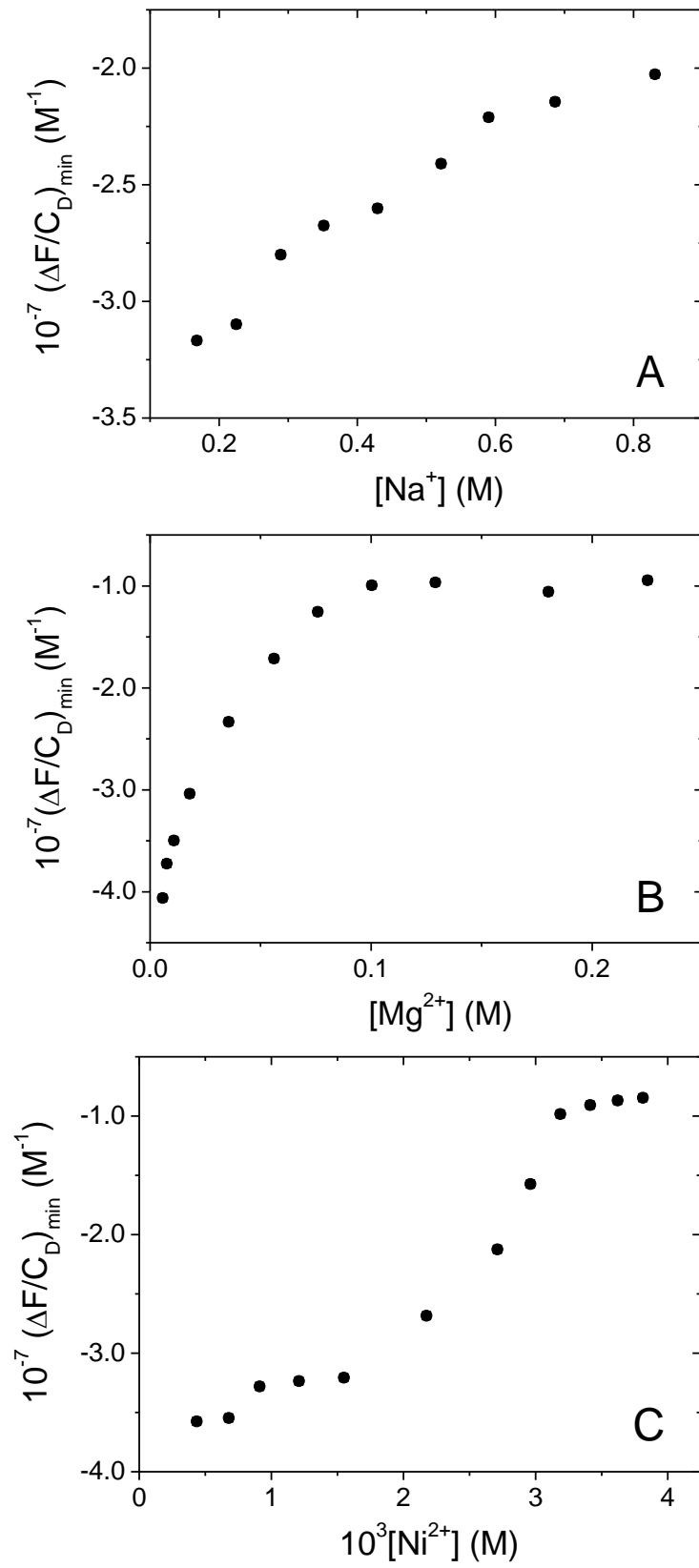


FIGURE 7

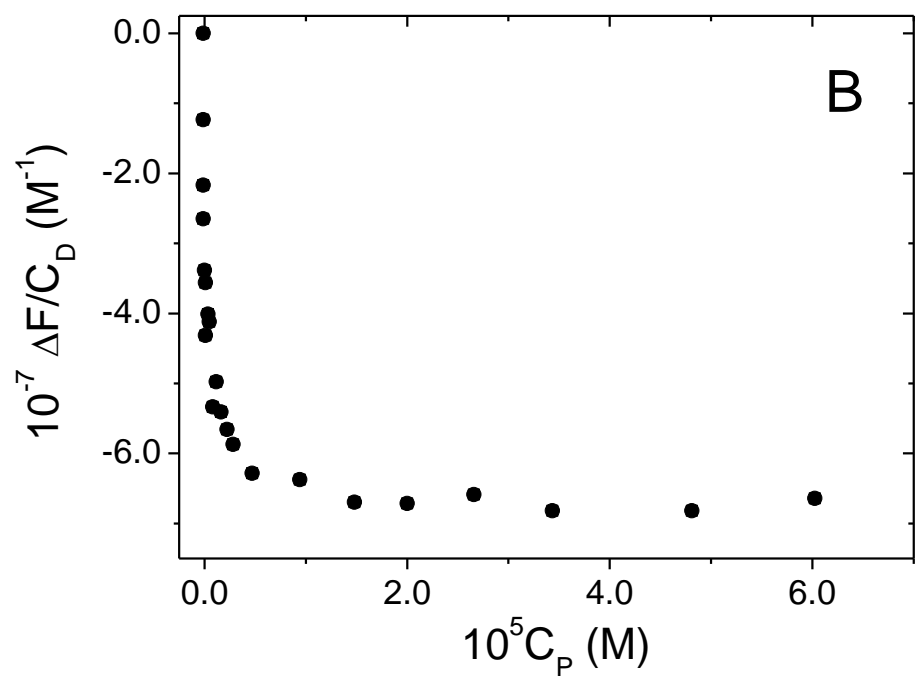
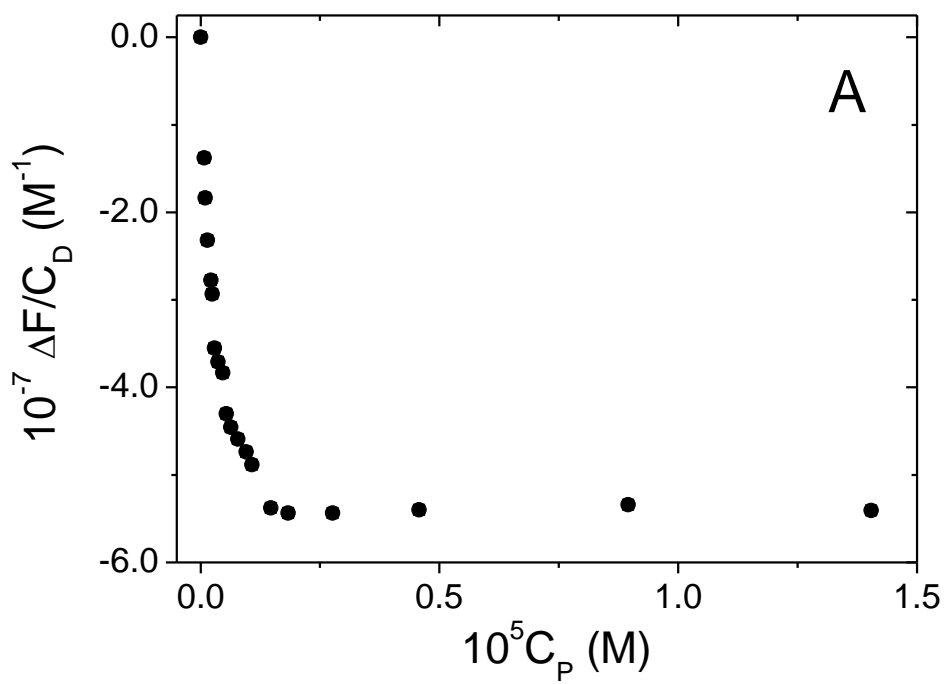


FIGURE 8

Figure1A
[Click here to download high resolution image](#)

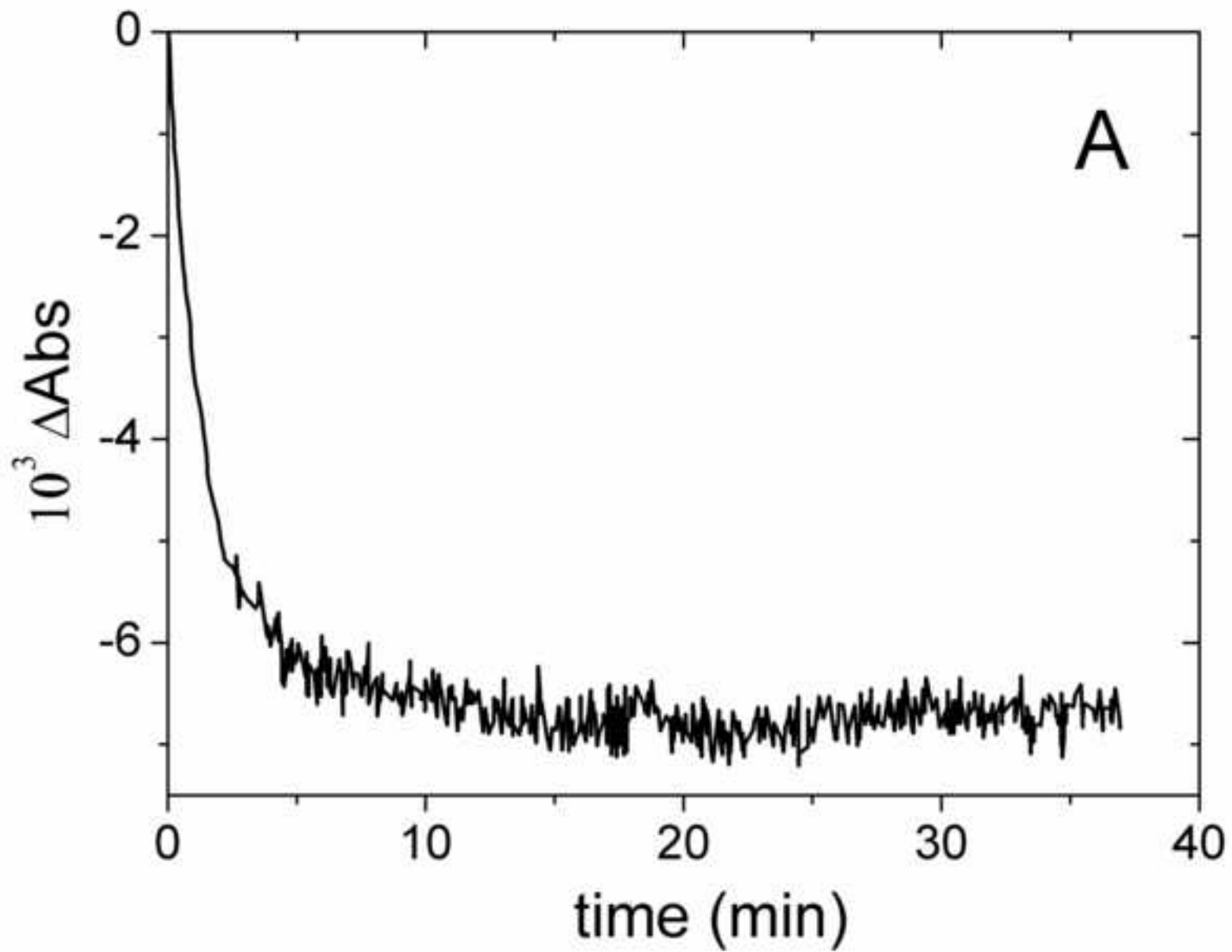


Figure1B
[Click here to download high resolution image](#)

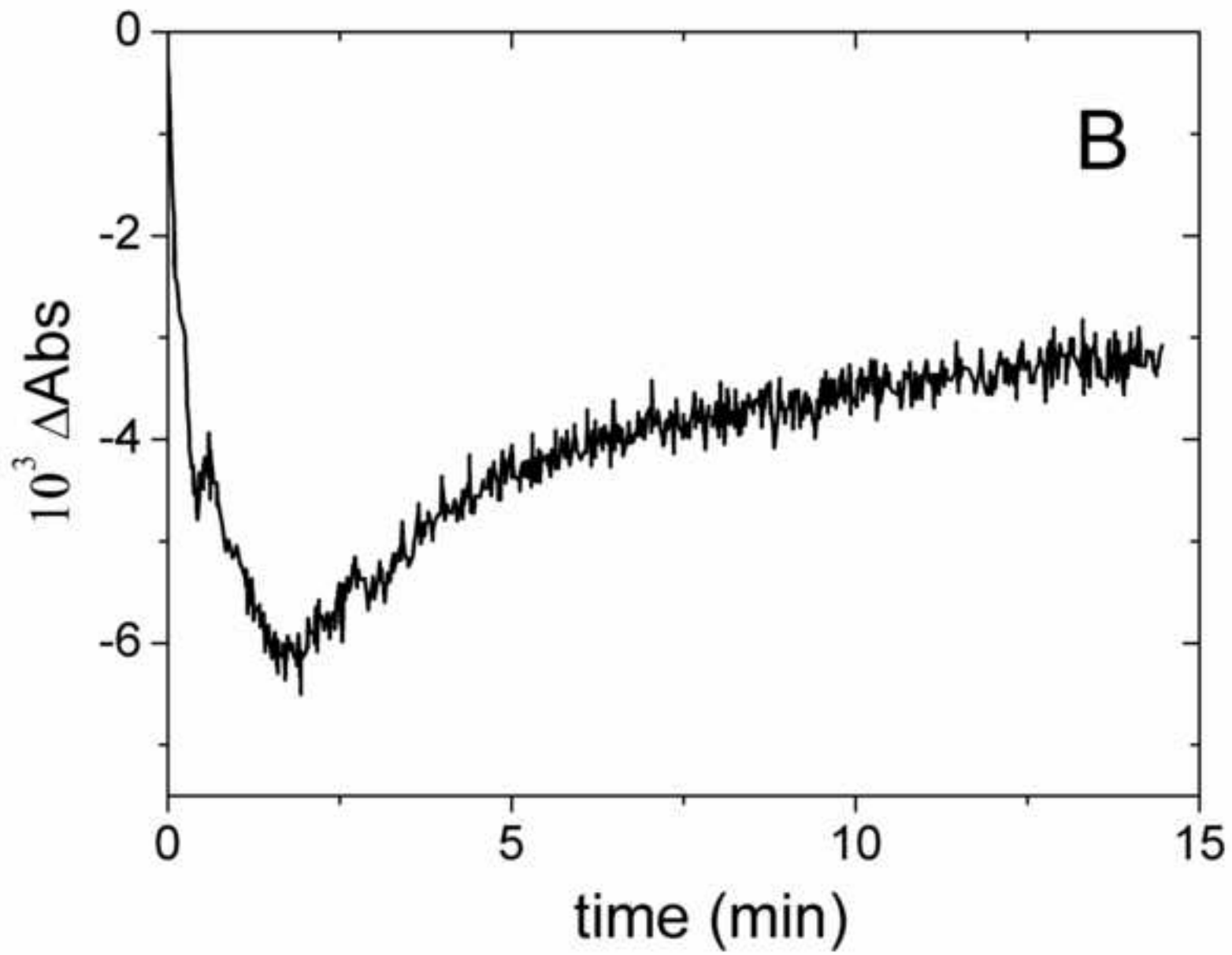


Figure1C
[Click here to download high resolution image](#)

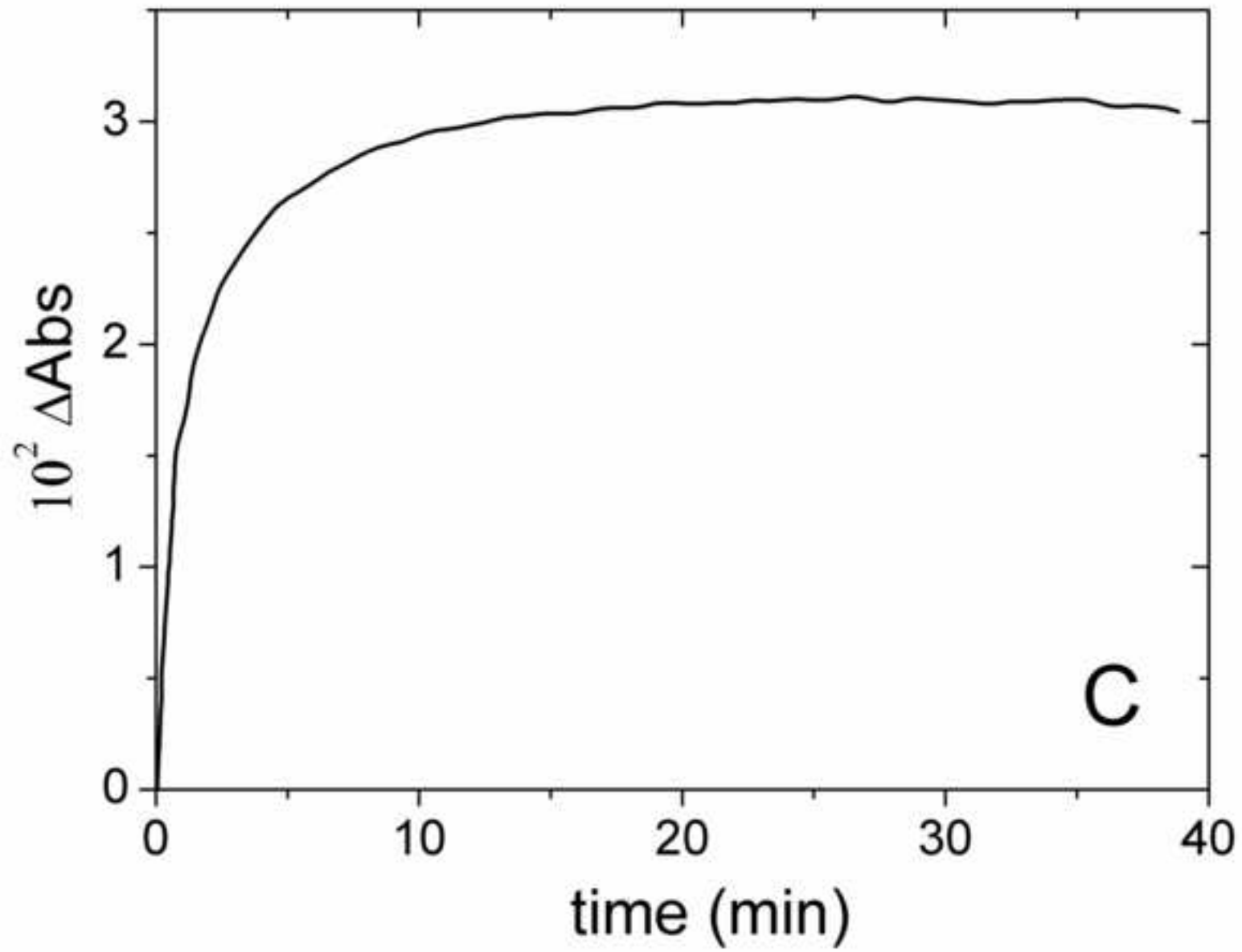


Figure2A
[Click here to download high resolution image](#)

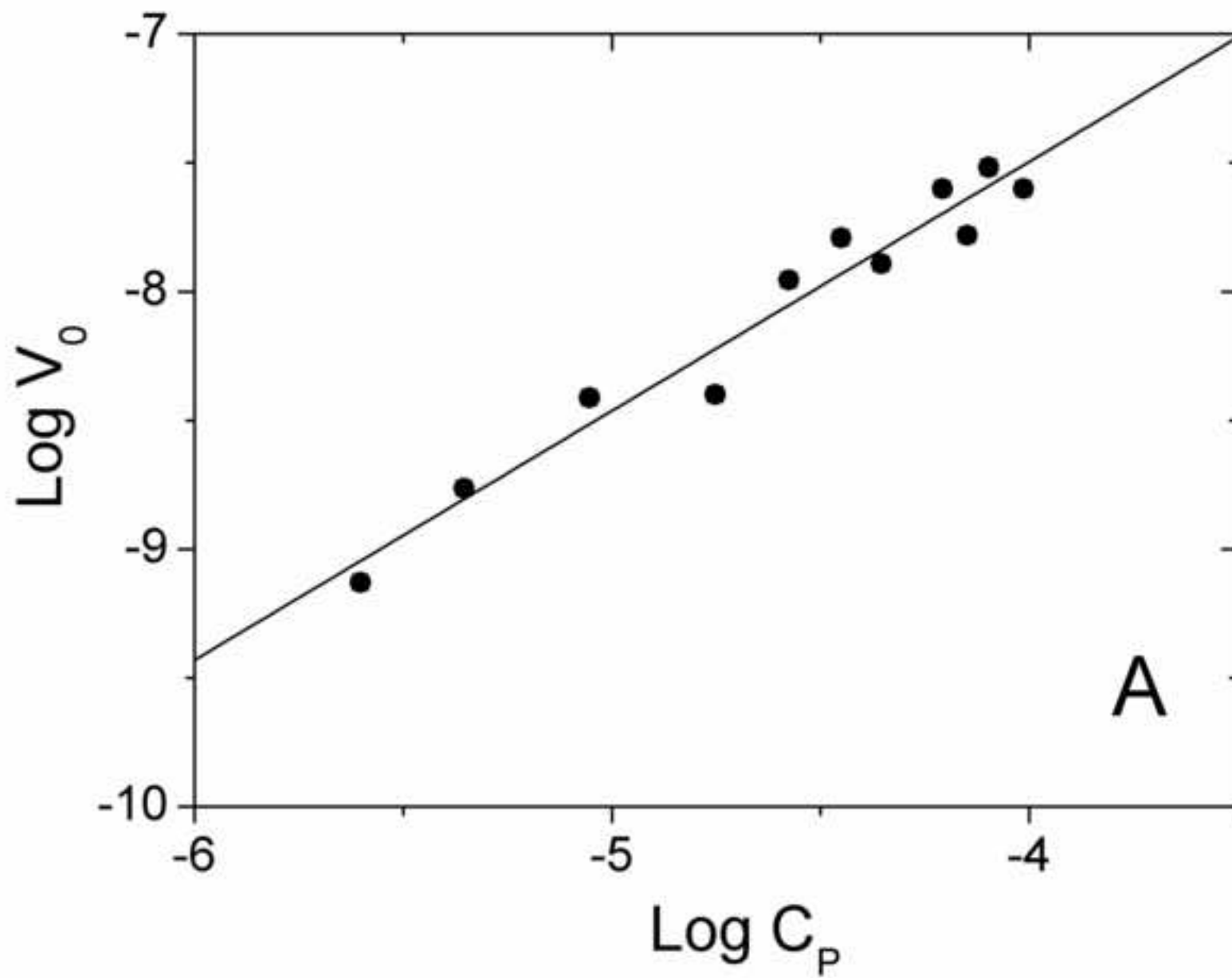


Figure2B
[Click here to download high resolution image](#)

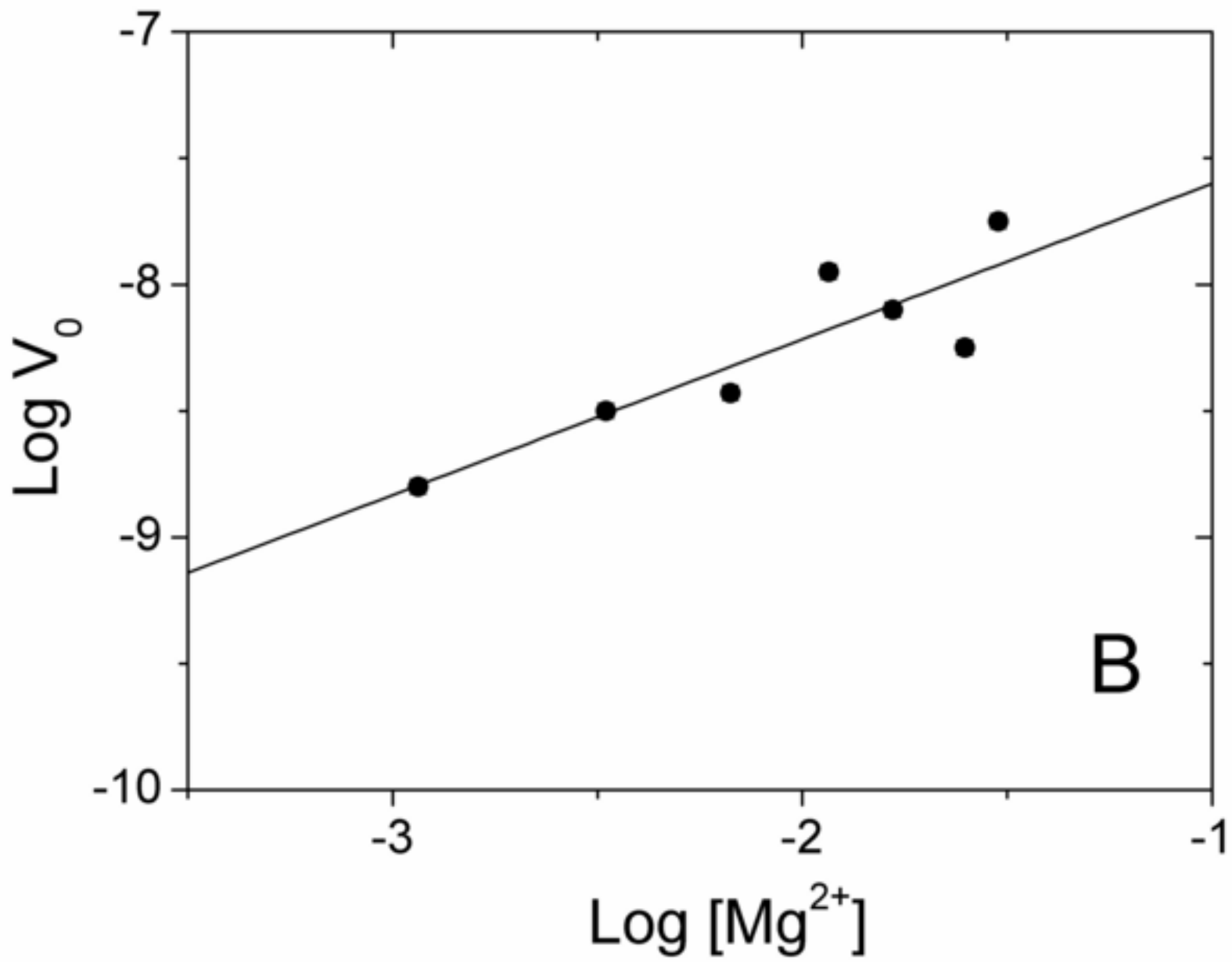


Figure3A
[Click here to download high resolution image](#)

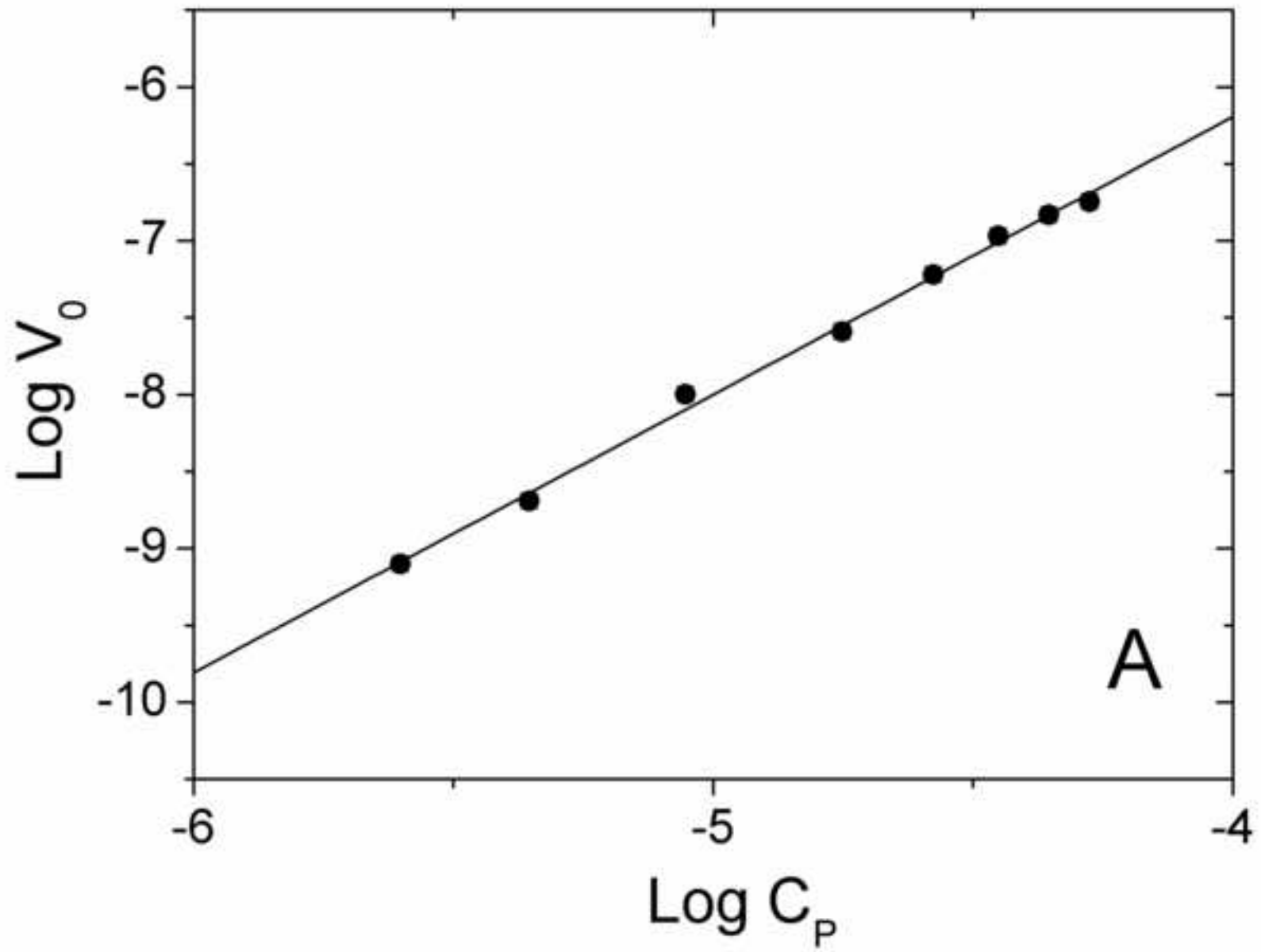


Figure3B
[Click here to download high resolution image](#)

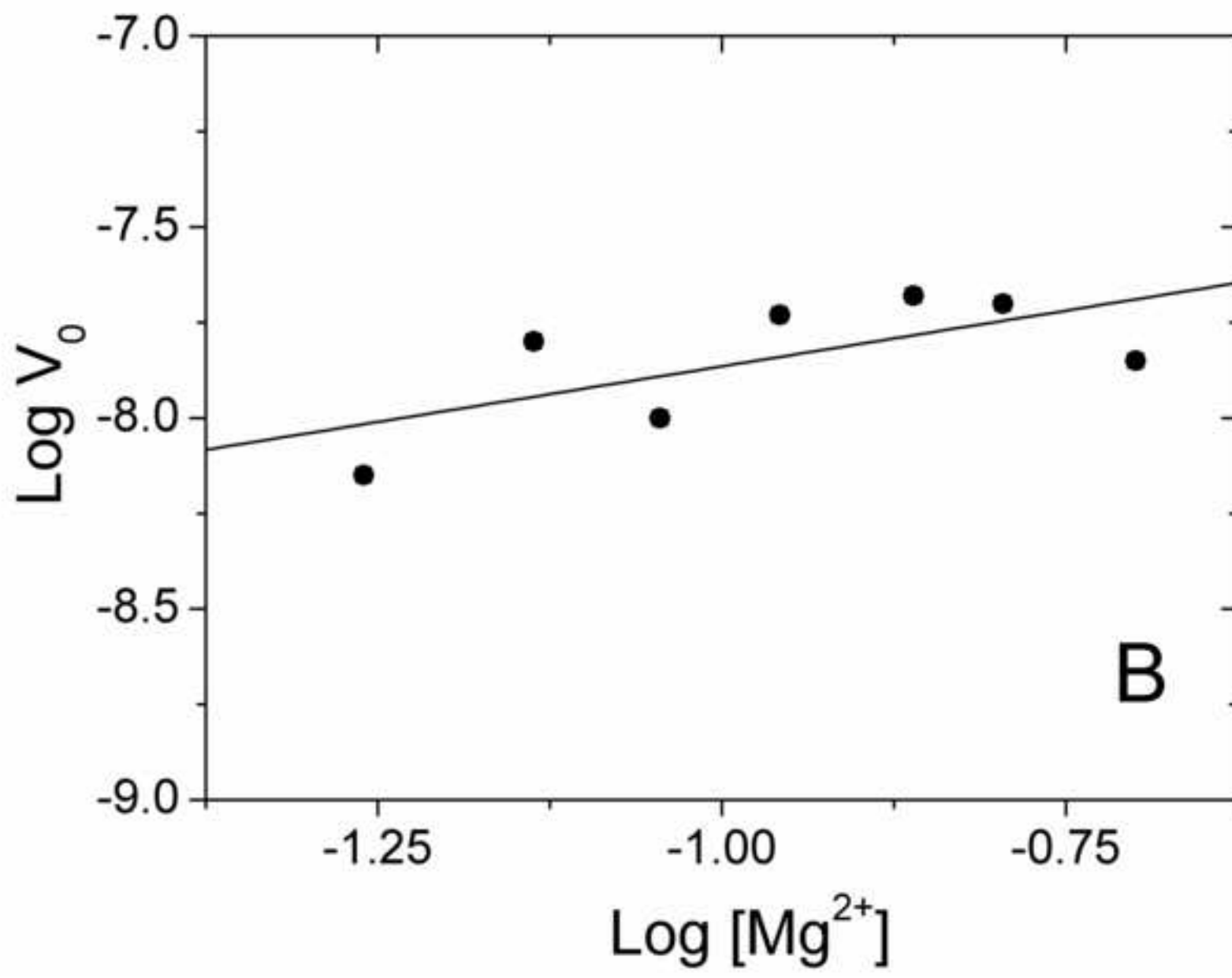


Figure4A

[Click here to download high resolution image](#)

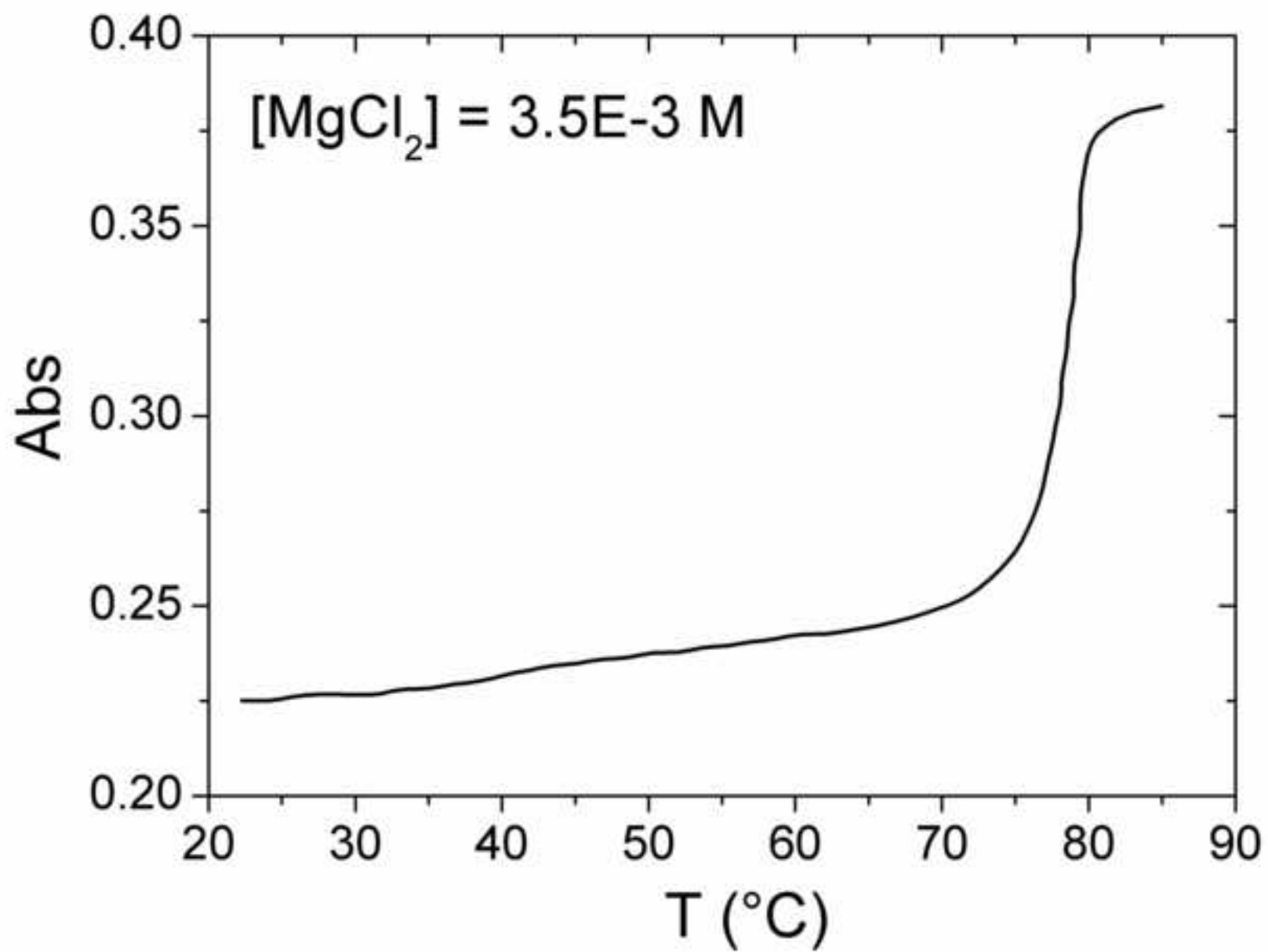


Figure4B

[Click here to download high resolution image](#)

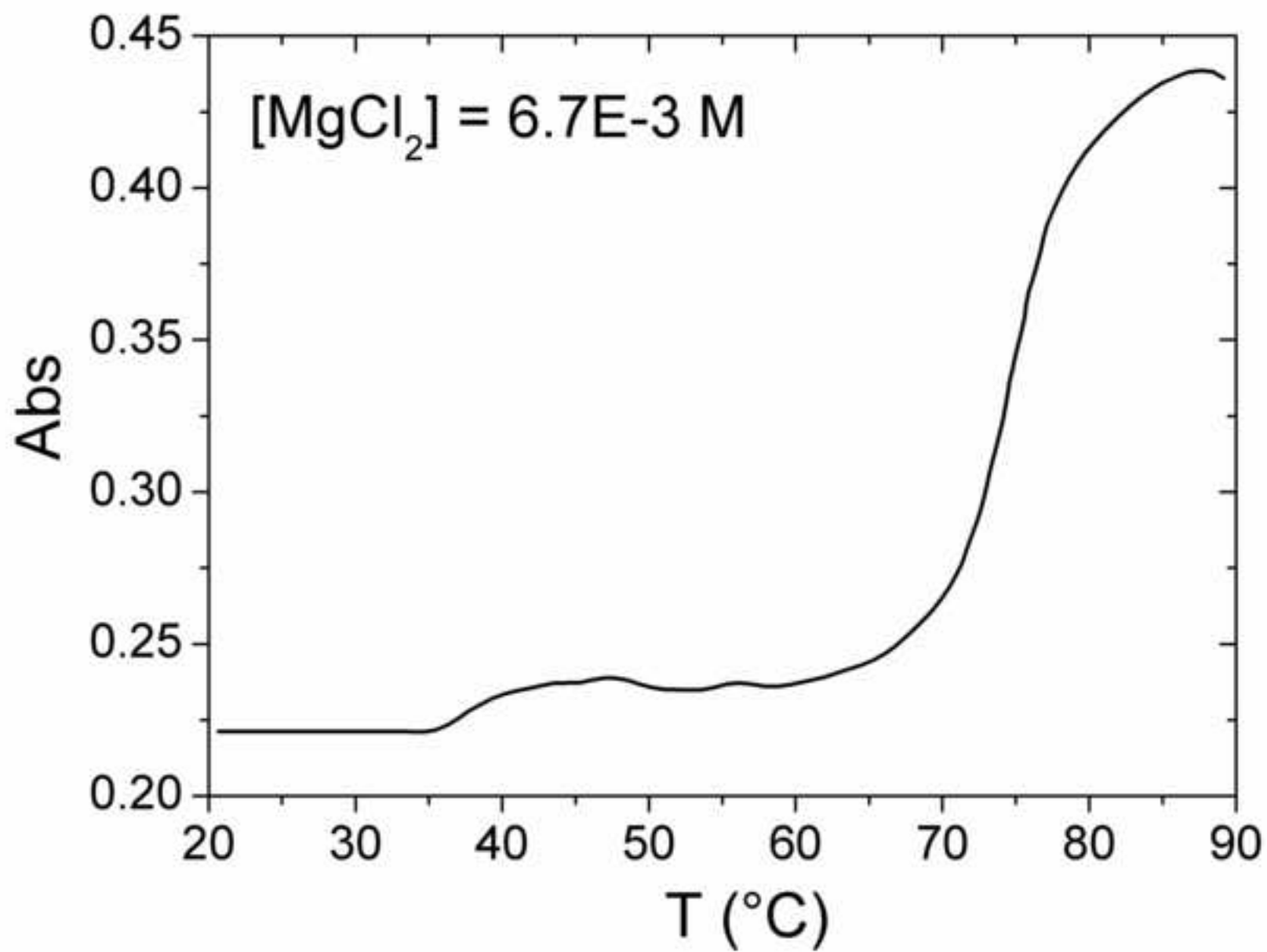


Figure4C

[Click here to download high resolution image](#)

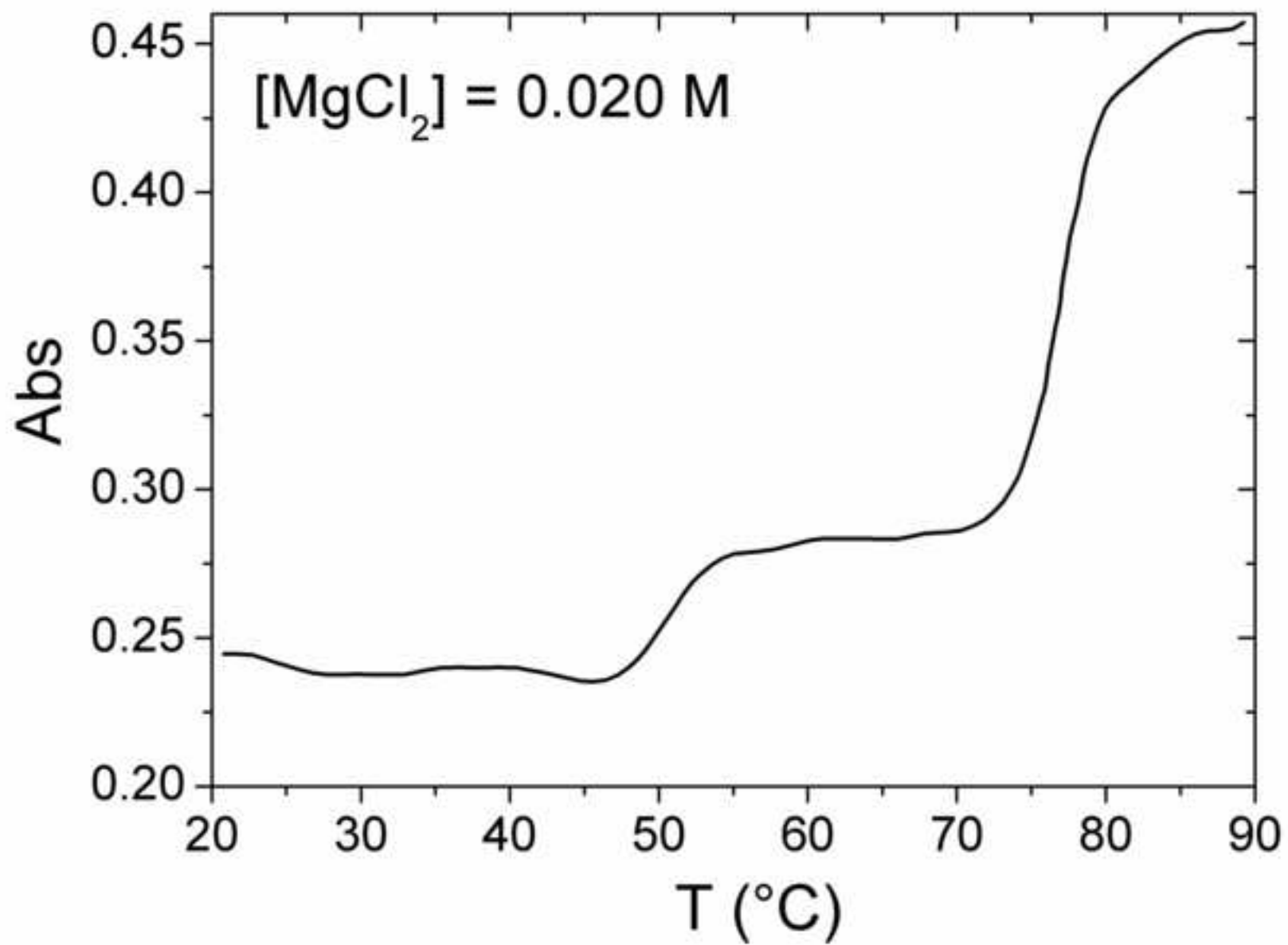


Figure4D

[Click here to download high resolution image](#)

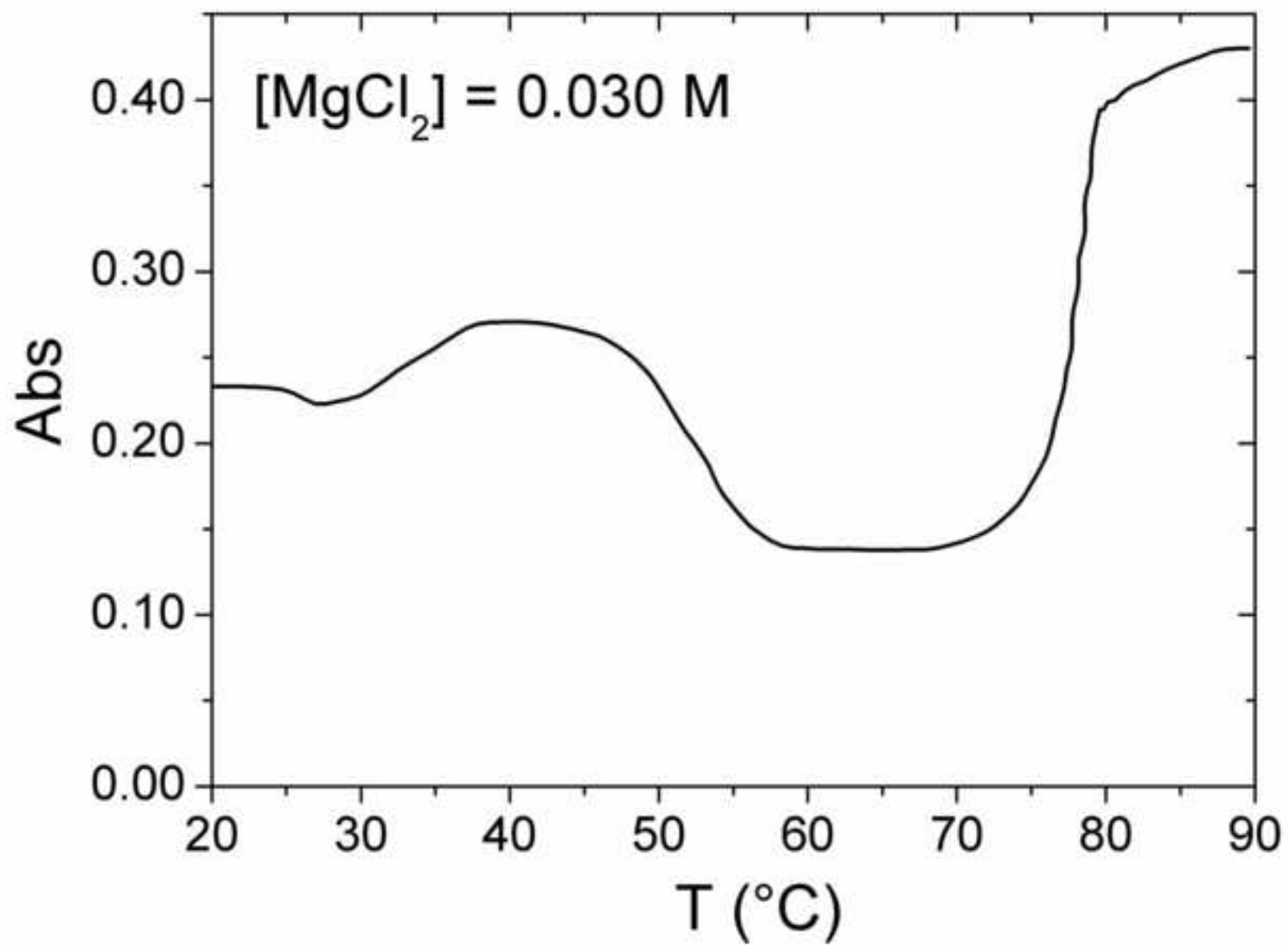


Figure4E

[Click here to download high resolution image](#)

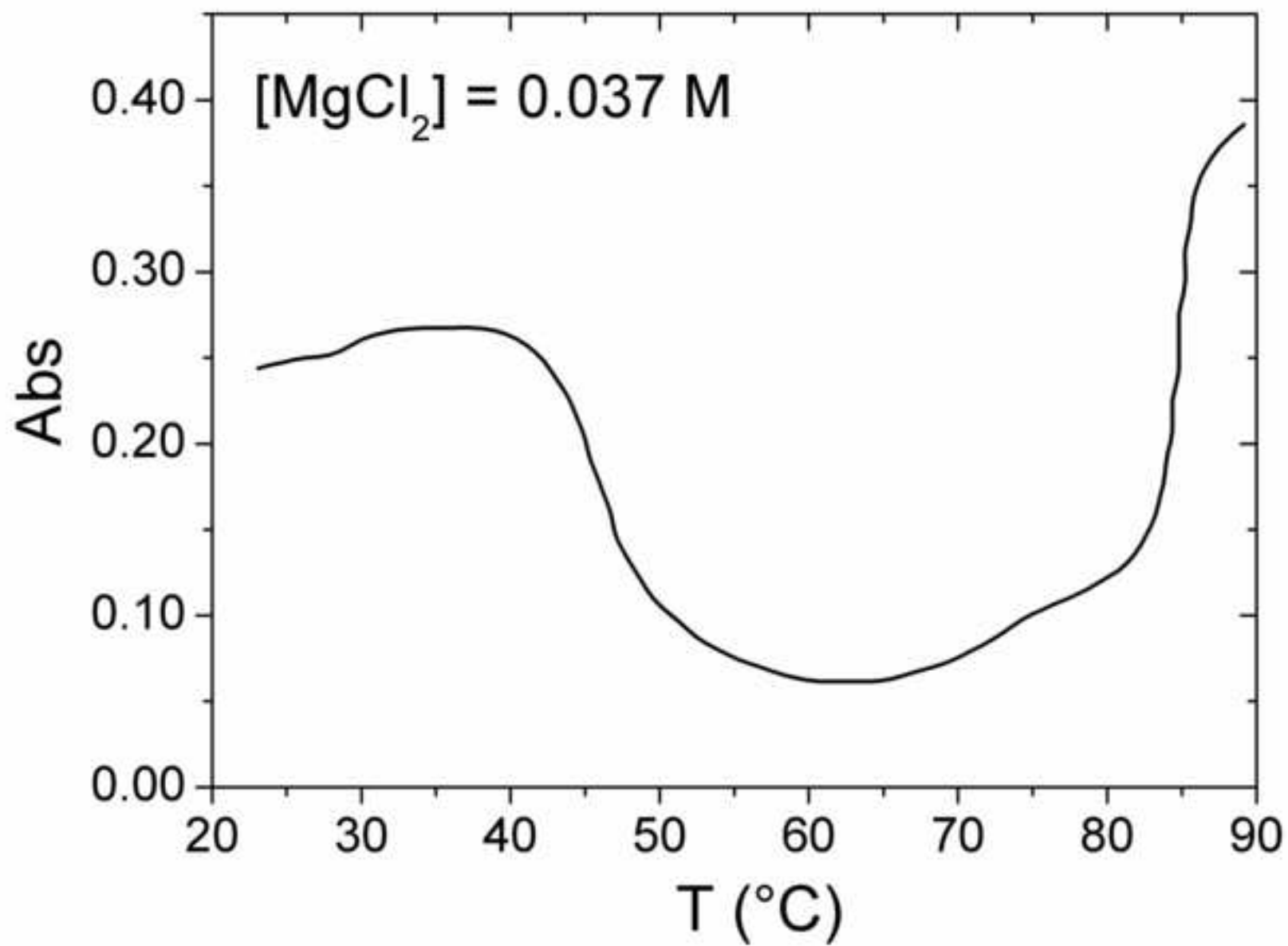


Figure4F

[Click here to download high resolution image](#)

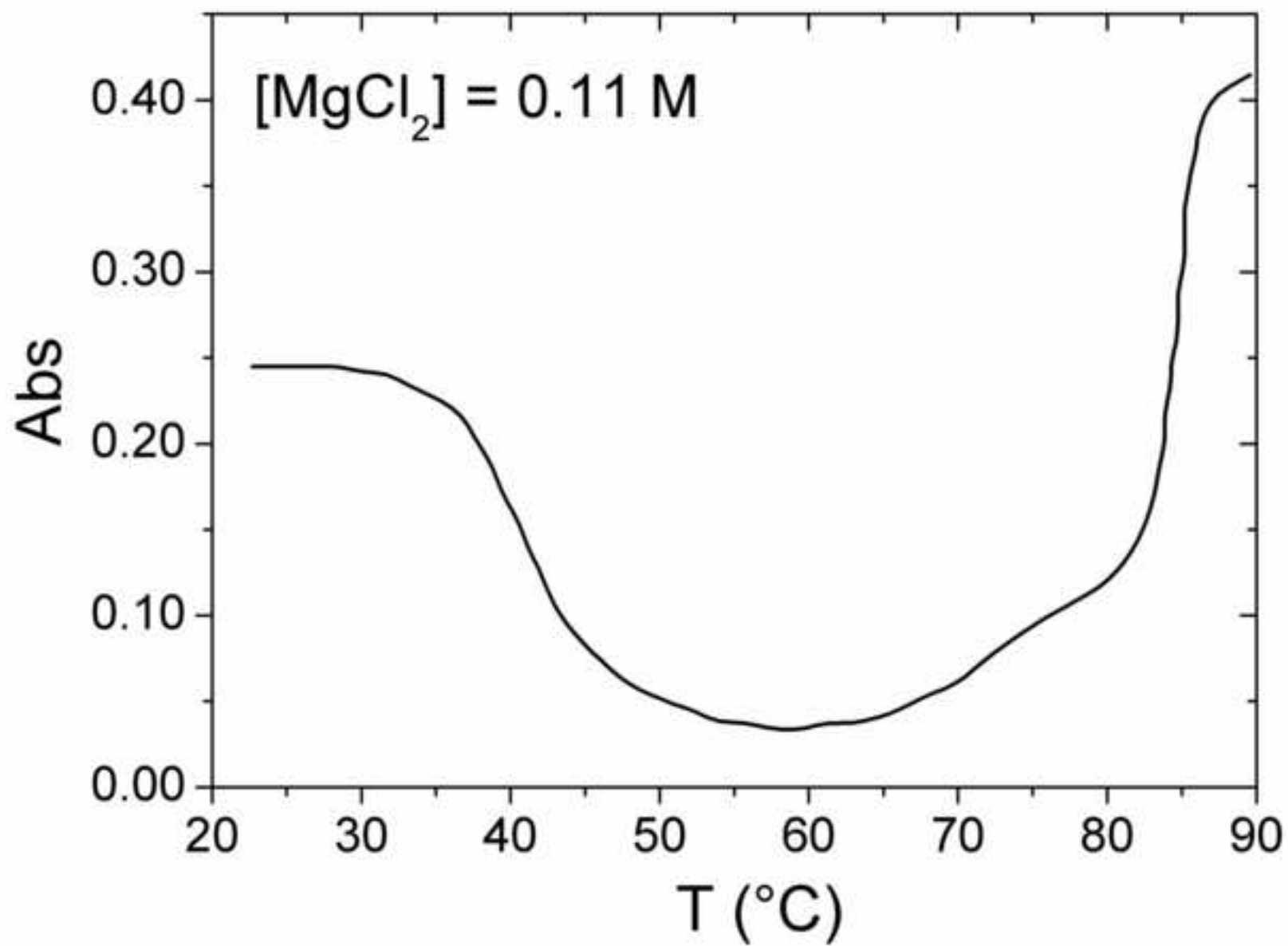


Figure5A
[Click here to download high resolution image](#)

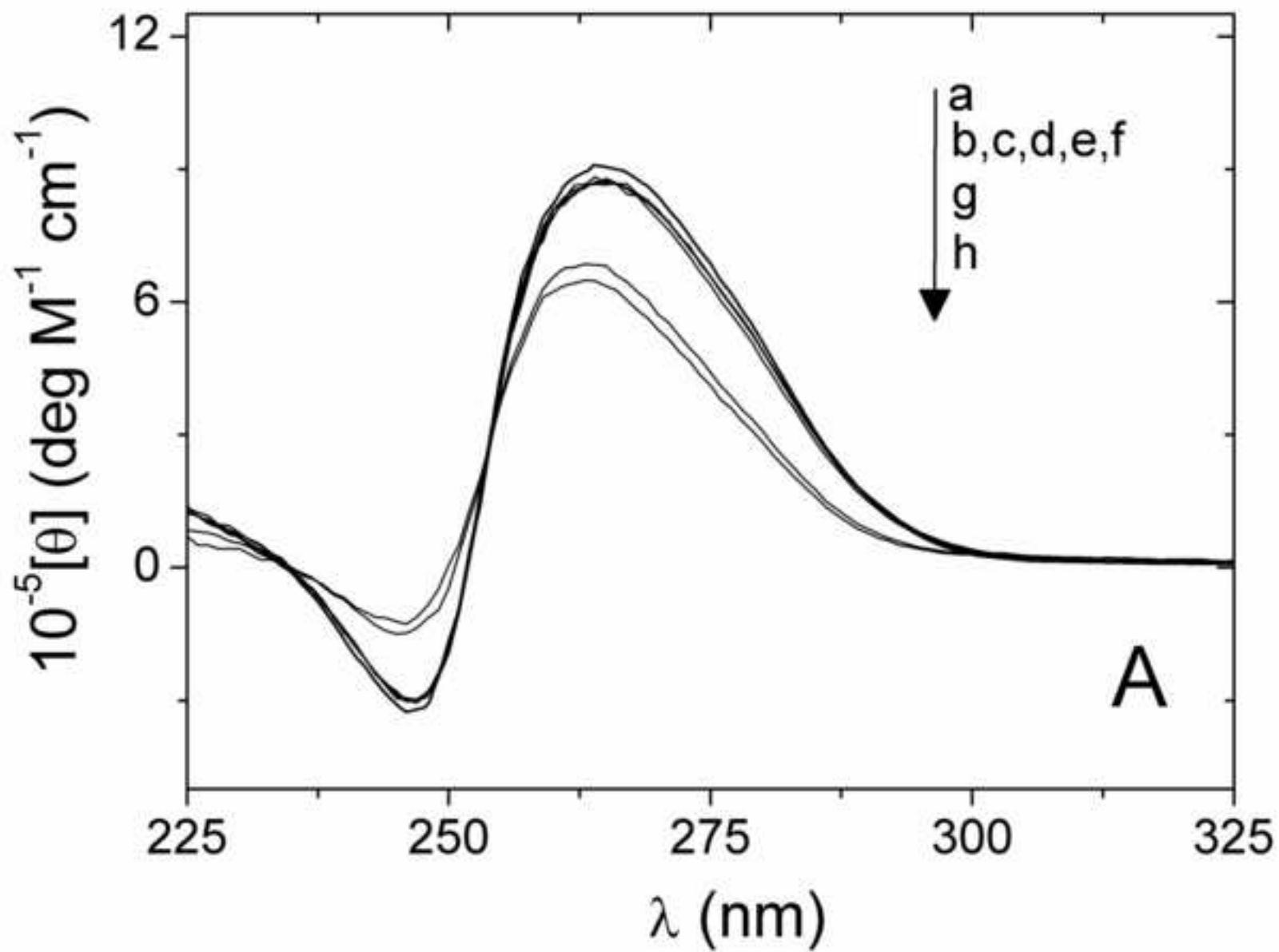


Figure5B
[Click here to download high resolution image](#)

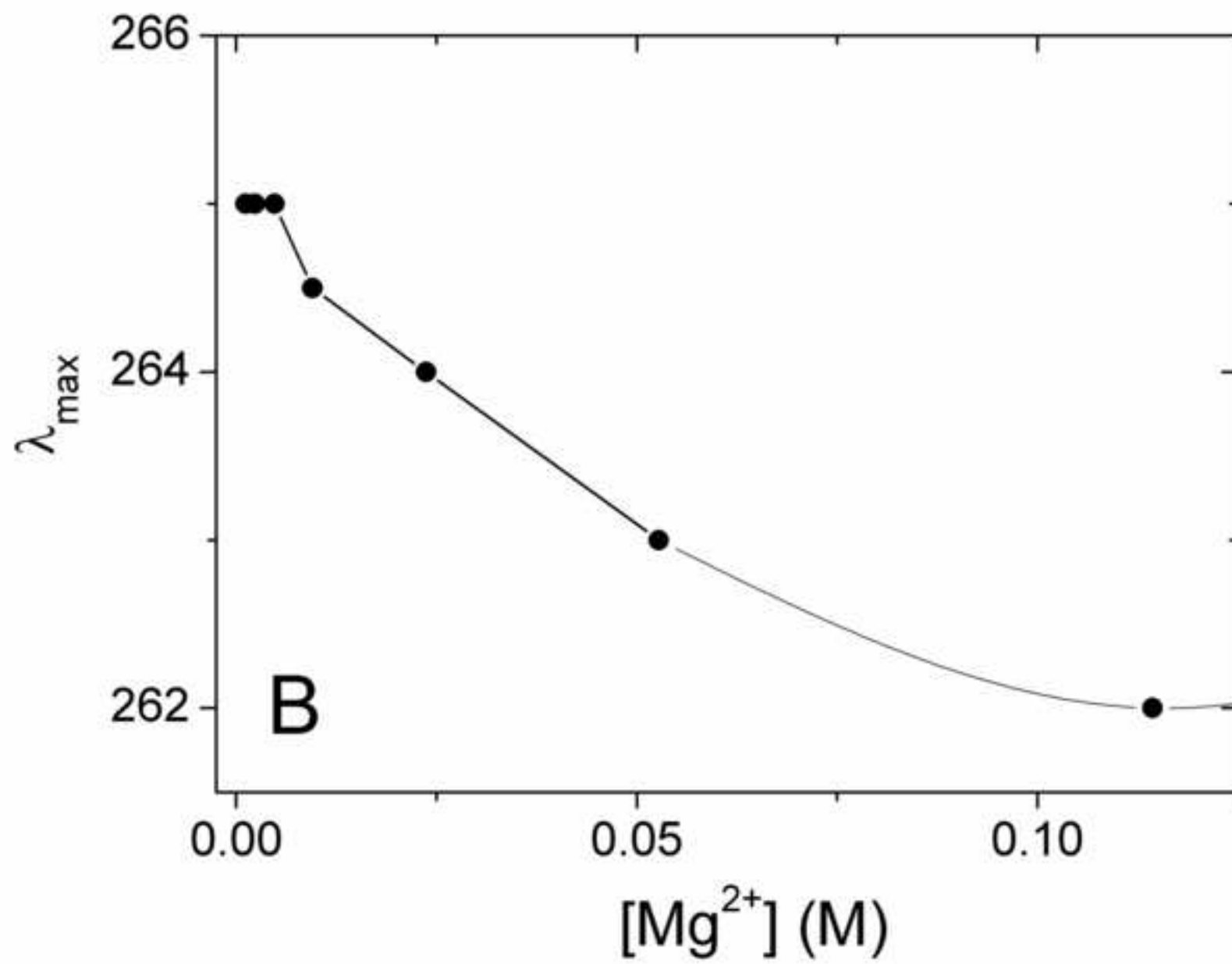


Figure6
[Click here to download high resolution image](#)

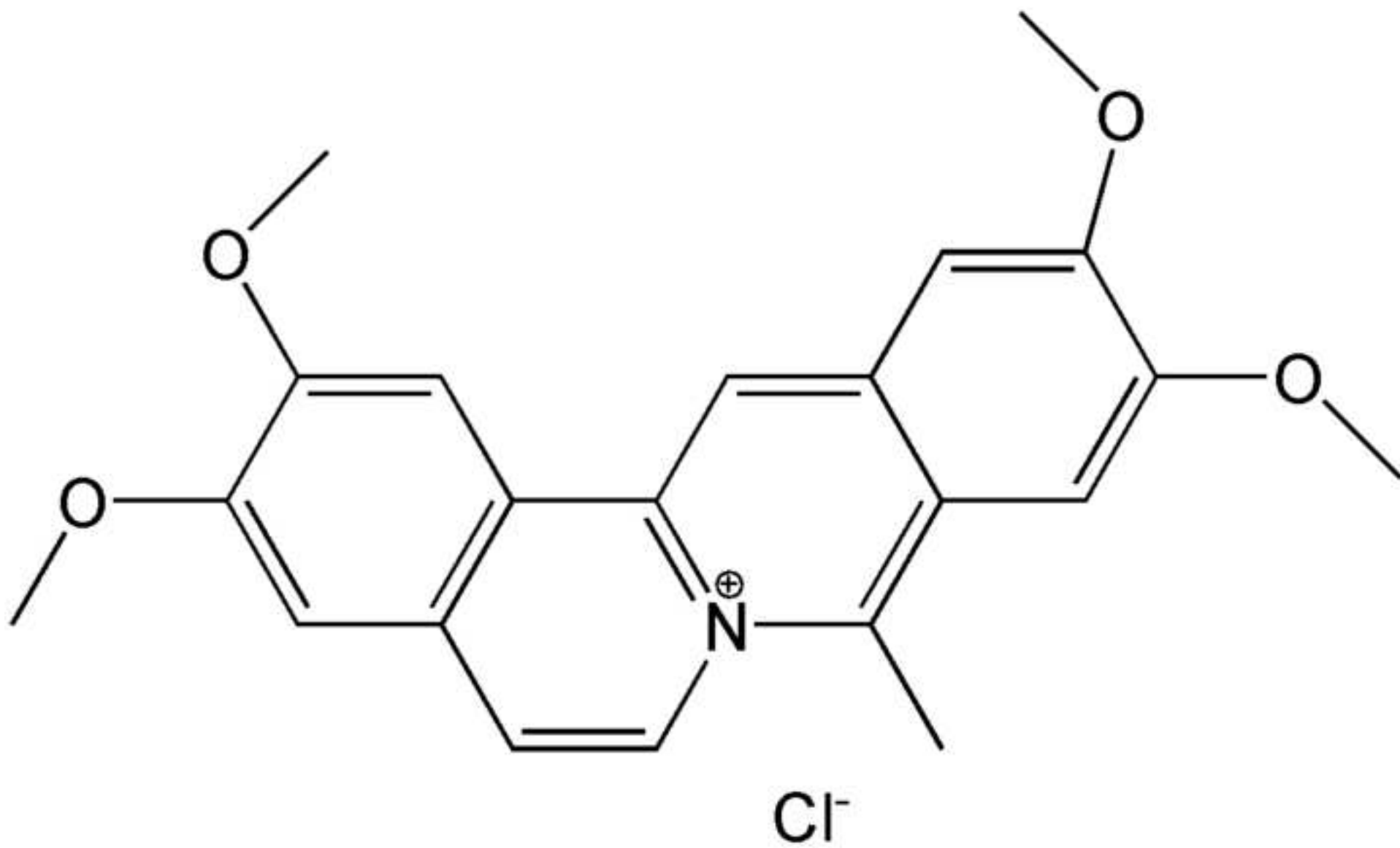


Figure7A
[Click here to download high resolution image](#)

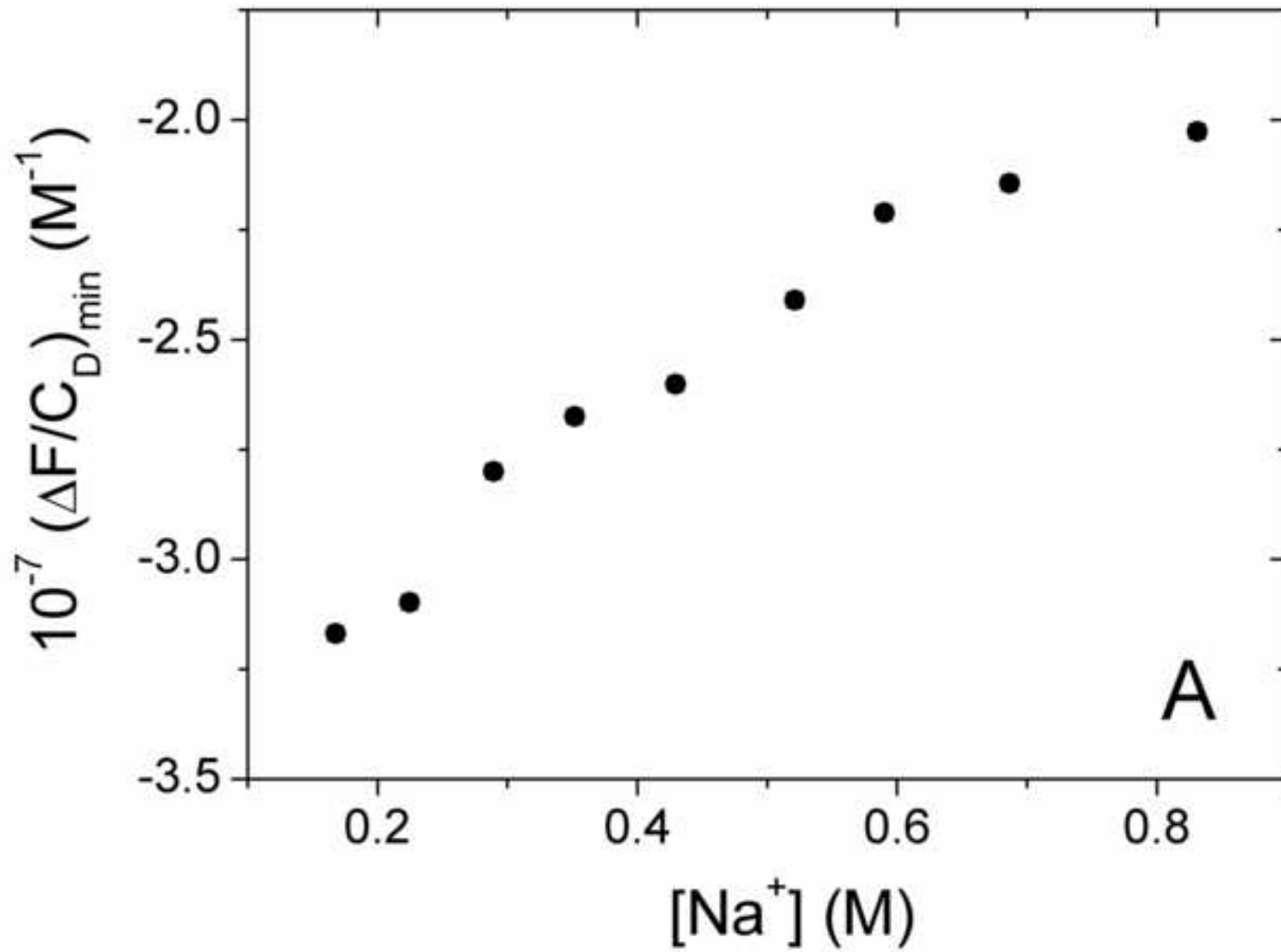


Figure7B
[Click here to download high resolution image](#)

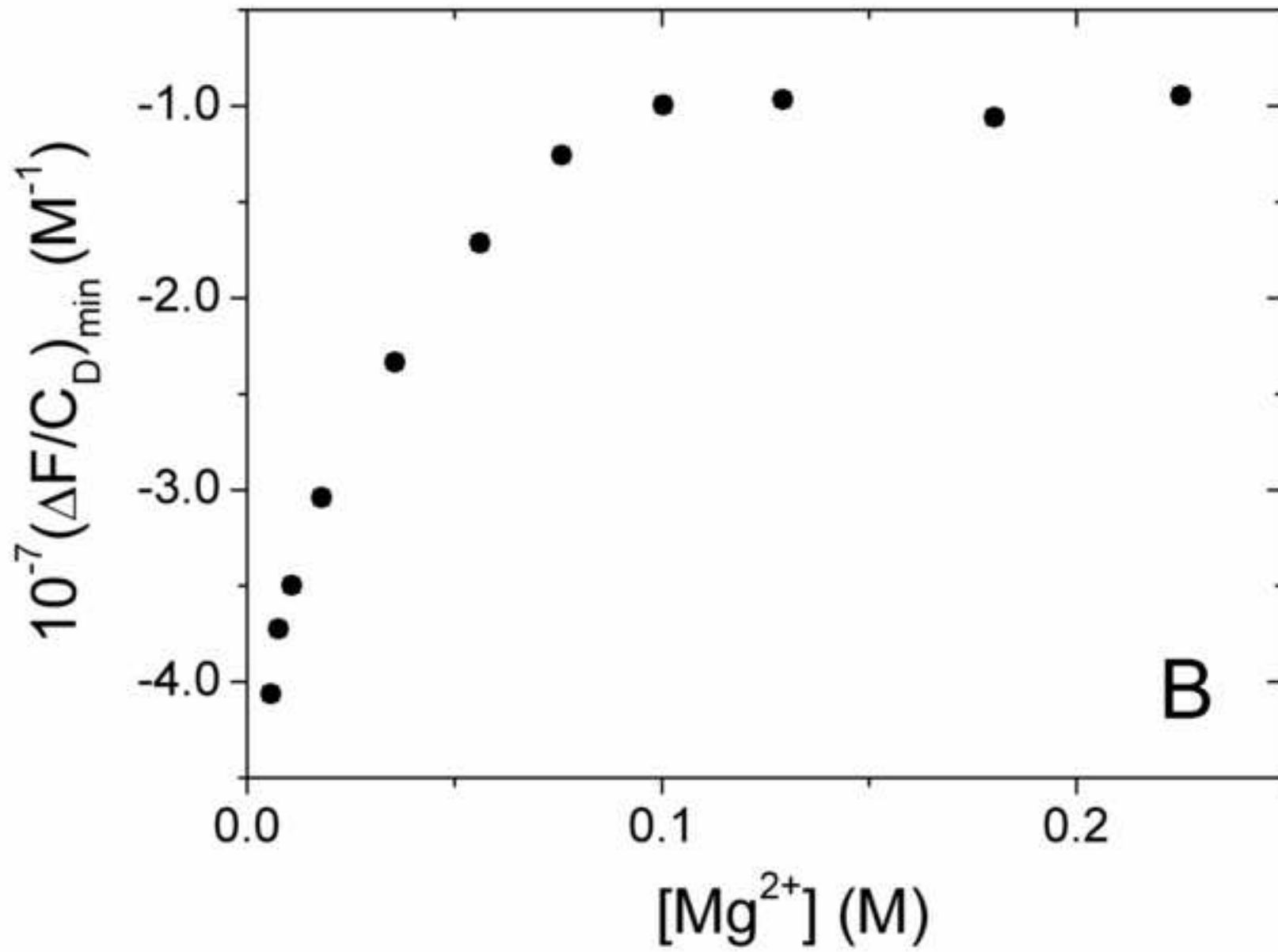


Figure7C
[Click here to download high resolution image](#)

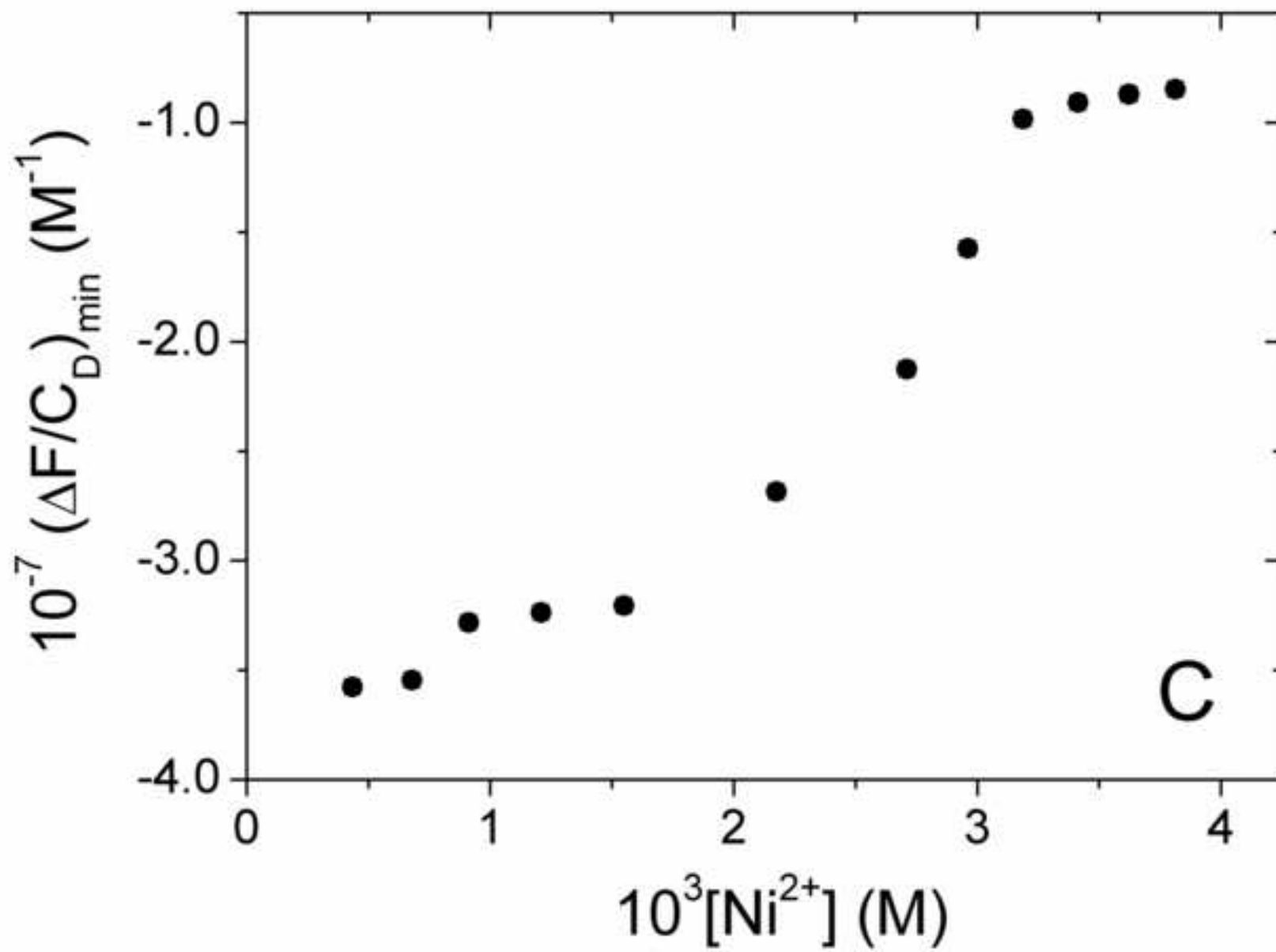


Figure8A
[Click here to download high resolution image](#)

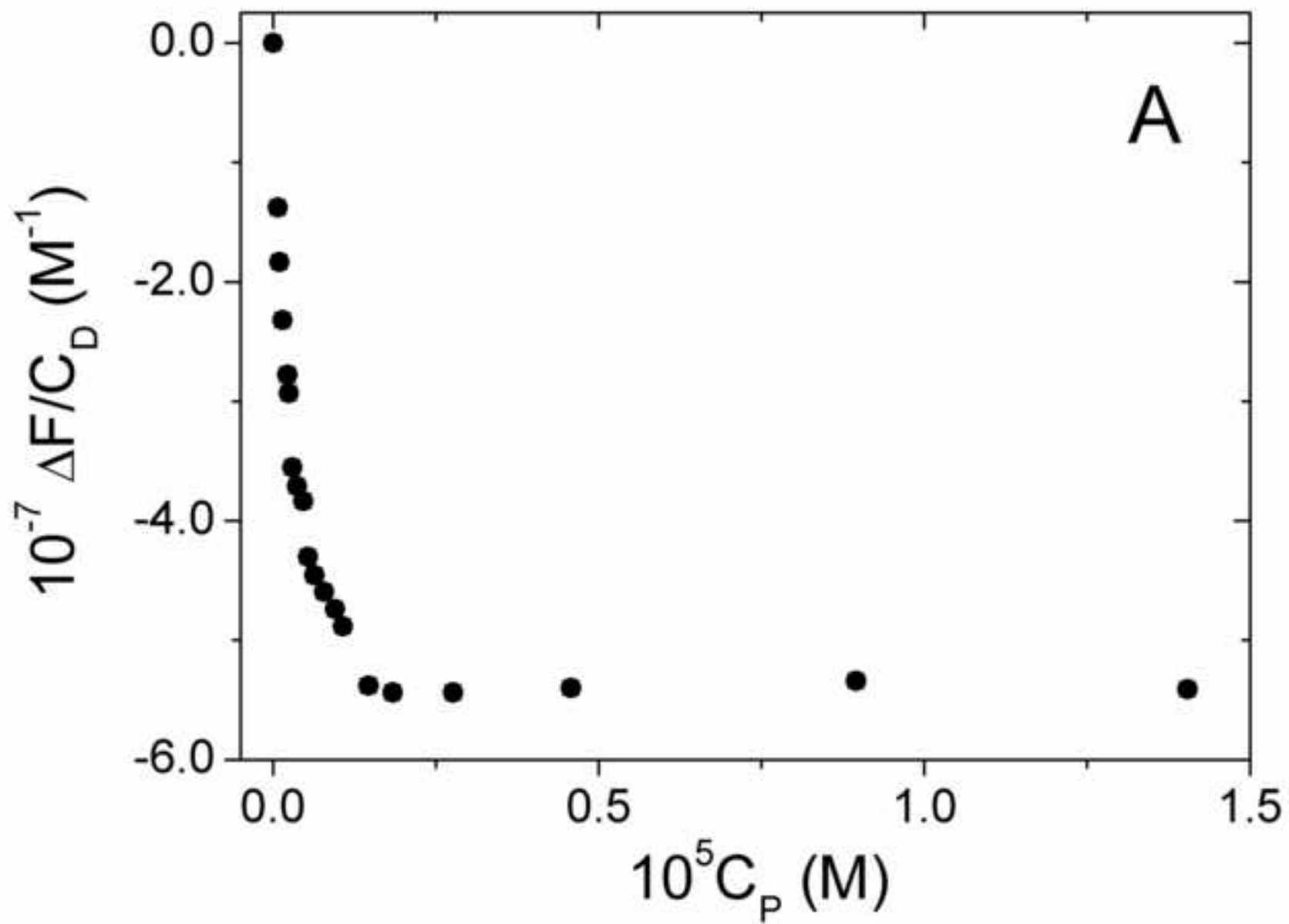
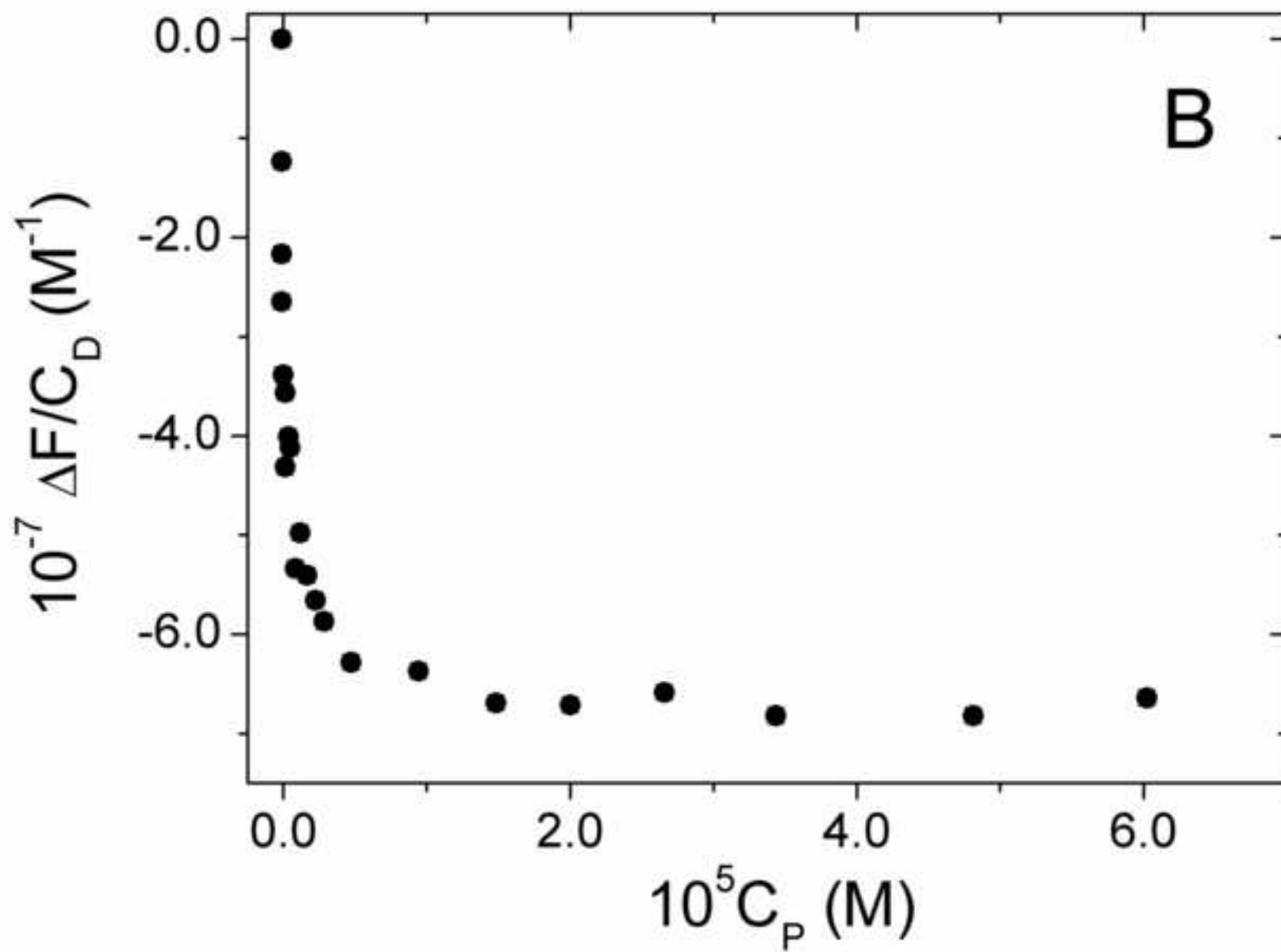


Figure8B
[Click here to download high resolution image](#)



Supplementary Information for Publication Online

[Click here to download Supplementary Information for Publication Online: SUPPORTING INFORMATION.pdf](#)